ENGINEERING Energy 2026, 20(1): 10446
https://doi.org/10.1007/s11708-026-1044-6

REVIEW ARTICLE

Progress and perspectives of electrochemical CO_2 reduction to methanol

Changlong Zhu[1,2,3], Xupeng Yan[1], Peng Liu (✉)[1], Qichen Lu[1], Lin Hu[1], Tianyi Zhou[1], Ruling Huang[1], Bo Hu[1], Kexin Zhang[1], Xiaolong Wang (✉)[1,4], Dongfang Guo[1,4], Shisen Xu[4,5], Qinggong Zhu (✉)[2,3], Buxing Han (✉)[2,3]

1 China Huaneng Clean Energy Research Institute, Beijing 102209, China
2 Beijing National Laboratory for Molecular Sciences, Key Laboratory of Colloid and Interface and Thermodynamics, Institute of Chemistry, Chinese Academy of Sciences, Beijing 100190, China
3 University of Chinese Academy of Sciences, Beijing 100049, China
4 National Key Laboratory of High-Efficiency Flexible Coal Power Generation and Carbon Capture Utilization and Storage, China Huaneng Clean Energy Research Institute, Beijing 102209, China
5 China Huaneng Group Co., Ltd., Beijing 100031, China

HIGHLIGHTS

- This review outlines findamentals and status of electrochemical CO_2-to-methanol conversion.
- It summarizes research progress across various electrocatalytic systems for methanol.
- Performance enhancement via photo-assisted and ionic liquid strategies is discussed.
- The current challenges and future research directions are highlighted.

Keywords:
Electrocatalysis
Carbon dioxide
Methanol
Catalysts
Electrolyte

ABSTRACT

The increasing emission of carbon dioxide (CO_2) has intensified global efforts toward its conversion and utilization. Electrocatalytic CO_2 reduction reaction (CO_2RR) has emerged as a promising sustainable strategy to address interconnected energy and environmental challenges. Among the various products of CO_2 reduction, methanol has attracted significant research attention as both an essential chemical feedstock and a promising renewable energy carrier. This review comprehensively summarizes recent advances in the electrocatalytic conversion of CO_2 to methanol, with systematic discussions on fundamental reaction mechanisms and pathways, innovative reactor configurations, diverse catalysts, and auxiliary optimization strategies. Particular emphasis is placed on categorizing and evaluating various catalysts, including mono-/bimetallic catalysts, molecular catalysts, enzyme catalysts, and carbon-based materials, while exploring their structure-activity relationships and performance enhancement strategies for improving methanol selectivity. Furthermore, the techno-economic viability of current processes is analyzed, assessing the cost-effectiveness and commercial potential of electrocatalytic methanol production. Finally, based on current research progress and existing challenges, key research directions are outlined to advance the development of commercially feasible electrocatalytic CO_2-to-methanol systems, providing practical guidance for future investigations.

1 Introduction

With accelerating global industrialization, a surging global population, and rapid civilization progress, energy demand has risen substantially. The large-scale use of fossil fuels has driven a sharp rise in CO_2 emissions [1]. The report "Global Carbon Balance 2024" indicates that global CO_2 emissions reached 41.6 billion tons in 2024, with fossil fuels emissions accounting for 37.4 billion tons. These excessive CO_2 emissions have triggered a series of severe environmental problems, including global warming, rising sea levels, and more frequent extreme weather events [2–4]. Concurrently, CO_2 has garnered increasing attention from researchers across diverse fields

✉ Corresponding authors. E-mails: p_liu@qny.chng.com.cn (P. Liu); xl_wang@qny.chng.com.cn (X. Wang); qgzhu@iccas.ac.cn (Q. Zhu); hanbx@iccas.ac.cn (B. Han)

Article history: Received 25 June 2025, Revised 4 August 2025, Accepted 20 October 2025, Available online 10 January 2026

due to its characteristics of non-toxicity, easy availability, and high recyclability. Converting emitted CO_2 into valuable resources and chemicals through capture and reduction processes represents a promising strategy not only for addressing current energy challenges but also for mitigating global warming [5–7].

The electrocatalytic CO_2 reduction reaction (CO_2RR), is a process that mimicks artificial photosynthesis by converting CO_2 into value-added chemicals using renewable electricity, utilizes an applied potential between electrodes to drive CO_2 reduction [8]. Recognized as a promising strategy for achieving carbon neutrality, this technique has been extensively studied due to its dual advantages of economic feasibility and environmental sustainability [9]. The electrocatalytic CO_2RR involves the sequential transfer of multiple electrons and protons, enabling the production of diverse products ranging from C_1 products (e.g., carbon monoxide, formate, and methanol) to multi-carbon species such as ethylene, ethanol, propanol, and acetate (Fig. 1) [10–13]. However, this intrinsic product diversity, stemming from complex reaction pathways, presents a significant challenge in achieving high selectivity toward specific target products. Crucially, the reaction selectivity and efficiency are critically determined by the interplay of multiple factors, including catalyst composition and structure, electrolyte properties, cell configuration, and applied potential [14–16].

Among the many products derived from CO_2RR, methanol stands out as a vital chemical feedstock and clean energy carrier. With an energy density of 15.6 MJ/L, methanol serves as an efficient fuel for fuel cells, offering advantages such as high energy density and clean combustion. These properties position it as a leading candidate to replace conventional fossil fuels [17]. In industrial applications, methanol demonstrates extensive versatility, not only as a precursor for key organic compounds, including formaldehyde, acetic acid, methylamine, but also as critical building block for synthesizing olefins and gasoline-grade fuels [18]. At present, industrial methanol production primarily relies on fossil-derived syngas, a process that emits substantial CO_2 (approximately 2.6 tons of CO_2 per ton of methanol). While direct electrocatalytic conversion presents a transformative pathway for sustainable methanol synthesis, simultaneously achieving high selectivity, industrially relevant current densities (> 200 mA/cm^2), and long-term operational stability remains a formidable challenge.

Catalyst design is crucial for electrochemical CO_2 reduction reactions, as material composition, structure, and mechanistic pathways dictate distinct catalytic performance profiles [19,20]. Under certain conditions, low-cost catalysts can facilitate the formation of valuable chemicals [21]. Strategic catalyst design thus enables cost-effective production of high-value products [22]. Currently, copper-based catalysts are the most widely studied and have received significant attention in electrocatalytic CO_2 to methanol research. Additionally, noble metal catalysts, molecular catalysts, enzyme catalysts, and homogeneous catalysts have emerged as promising alternatives owing to their unique advantages in this field [23].

This review encompasses the critical aspects of electrocatalytic CO_2 reduction to methanol, highlights recent research progress, identifies scientific challenges, and outlines future research directions toward commercial applications. It aims to provide the research community with a deeper understanding of the current state of the field, thereby fostering further innovation in electrocatalytic conversion of CO_2 to methanol.

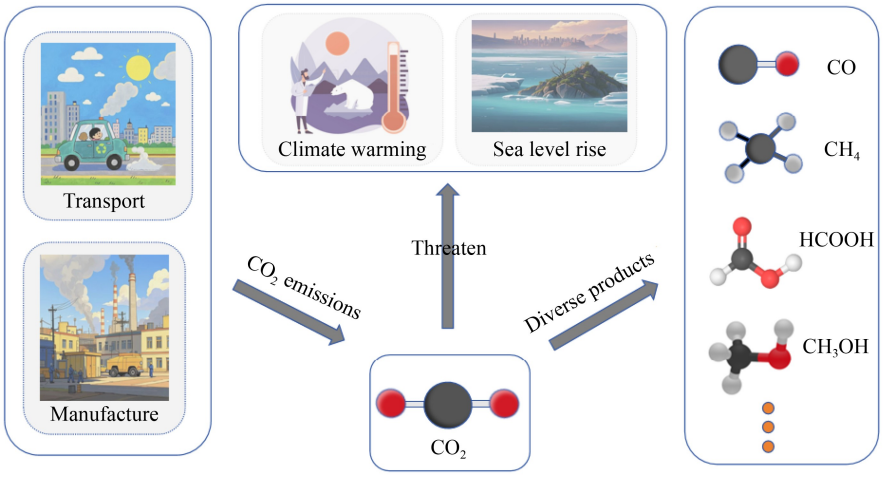

Fig. 1 Schematic illustration of CO_2 sources, threats, and various reduction products.

2 Fundamentals of electrocatalytic CO_2RR to methanol

The electrocatalytic reduction of CO_2 to methanol is an electrically driven process that utilizes CO_2 as feedstock and involves a six-electron/six-proton transfer [24]. The overall reaction can be represented as:

$$CO_2 + 6H^+ + 6e^- \rightarrow CH_3OH + H_2O$$

Typically, this complex process can be briefly summarized in four key stages:

1) adsorption and activation of CO_2 molecules on the catalyst surface;

2) proton-coupled electron transfer (PCET) generating reaction intermediates;

3) transformation of these intermediates;

4) formation of methanol [25].

However, achieving efficient CO_2 reduction to methanol remains a significant challenge. First, the reduction potential of CO_2 is close to that of the hydrogen evolution reaction (HER), leading to strong competition between the two processes [26]. Second, the highly stable C=O bond in CO_2 requires substantial energy input to break. In addition, the entire reaction process involves multiple electron-transfer steps and complex intermediate transformations, making it difficult to kinetically control intermediates and enhance methanol selectivity [27].

Catalysts play a crucial role throughout the entire reaction process by forming specific chemical bonds with CO_2 molecules, thereby lowering the energy required for CO_2 activation. Different catalysts exhibit varying catalytic activities in the PCET. These variations, determined by the type and properties of the catalyst, influence CO_2 adsorption patterns, reaction rates, product selectivity, and the subsequent reaction pathways leading to methanol generation [28]. In CO_2 reduction research, both photothermal catalysis and electrocatalysis have demonstrated significant advances [29].

Figure 2(a) illustrates the generalized CO_2RR-to-CH_3OH pathway common to most catalysts. Following adsorption and activation, CO_2 undergoes a PCET step to form the *COOH intermediate. This *COOH intermediate then accepts an electron and a proton to formic acid

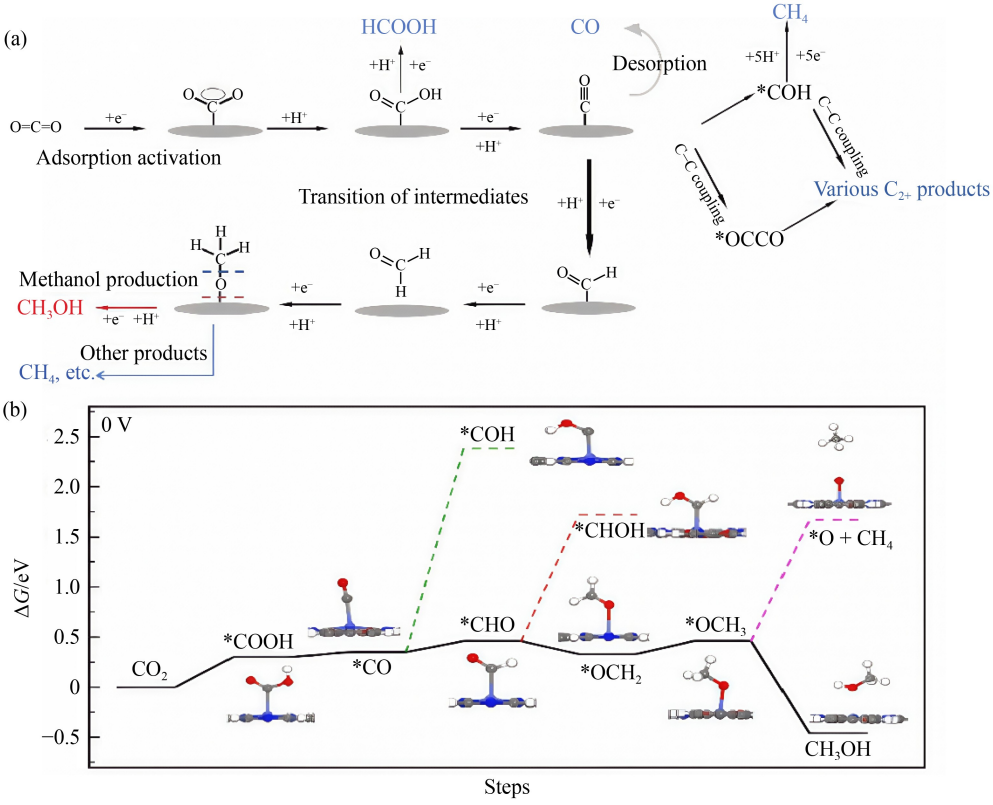

Fig. 2 Schematic illustration of the reaction pathway and energy profile for electrocatalytic CO_2 reduction to methanol, showing key intermediates and steps involved in the process.

(a) Simplified reaction mechanism for CH_3OH production from CO_2RR; (b) thermodynamically favorable reduction pathway (solid line) from CO_2 to CO and to CH_3OH. (Other competing pathways (dash lines) are also depicted.) (reproduced with permission from Yao et al. [31], copyright 2018, Wiley).

or is converted to the *CO intermediate. *CO represents a very critical reaction intermediate, as subsequent reaction pathways determine the final product distribution. Specifically, *CO desorb as gaseous CO or undergo hydrogenation to *CHO or *COH intermediates, both of which favor CH_3OH and CH_4 formation, respectively [30]. The *CO and *COH intermediates are also susceptible to C−C coupling, which tends to produce a variety of multi-carbon products.

The typical pathway for methanol production involves the sequential hydrogenation of the *CO intermediate through intermediates such as *CHO, $*CH_2O$, and $*CH_3O$, ultimately leading to methanol formation via hydrogenation and desorption from the catalyst surface to obtain the final product. Taking the Co-Pc-PBBA catalyst (PBBA = 1,4-phenylene diboraic acid) as an example, the CO_2 reduction process can be analyzed from the perspective of thermodynamic energy barriers (Fig. 2(b)) [31]. The entire methanol formation process exhibits a thermodynamic tendency toward spontaneous progression. However, distinct energy barriers must be overcome for each reaction intermediate, and the formation of alternative products poses a major challenge. Consequently, optimal reaction conditions and catalyst design are required at every stage to ensure efficient progression throughout the entire process.

During the progressive conversion of CO_2 to methanol, the adsorption energy of intermediates serves as a fundamental descriptor linked to catalytic activity, exerting a certain influence on methanol selectivity. For instance, a moderate *CO adsorption energy helps prevent desorption to CO while reducing the occurrence of C–C coupling that leads to multi-carbon products. However, the overall reaction pathway involves the transformation of multiple intermediates and multi-step PCET processes. Across different catalytic systems, the adsorption energies of reaction intermediates and the associated PCET energy barriers vary substantially. Furthermore, complicating factors such as solvent effects complicate quantitative predictions of methanol selectivity, making it difficult to identify universal descriptors applicable across diverse catalytic systems.

Currently, insights can be drawn from descriptors developed for other electrocatalytic processes. Among these, the d-band center is the most widely used descriptor, as it quantitatively captures interactions between the catalyst surface and adsorbates. By modulating the d-band center of active metal sites through strategies such as alloying or introducing defects, it is possible to tailor the electronic structure of the catalyst and enhance its performance. Additional types of descriptors include intrinsic property descriptors, which use readily accessible parameters such as electronegativity, coordination environment, and atomic radius to develop predictive models of catalytic activity. Moreover, spin property descriptors and multi-feature descriptors have shown promise in studies of reactions such as OER and HER [32]. These approaches offer valuable insights for developing suitable descriptors in the electrocatalytic conversion of CO_2 to methanol.

A comprehensive understanding of the electrocatalytic reaction process and mechanism enables a holistic view of the CO_2 conversion pathway. The formation of the key *CO intermediate and the precise control of subsequent reaction pathways will remain major focal points for future research.

3 Electrochemical cell configurations of CO_2RR to methanol

To realize an efficient CO_2RR process, researchers have developed various electrochemical cell configurations, primarily including H-type cells, gas diffusion electrolyzers, and membrane electrode assemblies (MEAs) [33]. Each configuration exhibits distinct structural, operational, and performance characteristics, making them suitable for different research or industrial applications. This section provides a brief introduction to these systems.

Schematic diagrams of typical electrochemical cell configurations are shown in Fig. 3. As depicted in Fig. 3(a), the H-type cell is a conventional device consisting of two separate chambers, the cathode chamber and the anode chamber, connected by an ion-exchange membrane or salt bridge. The cathode chamber is typically filled with a CO_2-saturated electrolyte solution (e.g., aqueous $KHCO_3$), which is in direct contact with the electrode. The anode chamber contains an electrolyte primarily used for the oxidation reaction of water (OER). During the CO_2RR process, CO_2 is first dissolved in the cathodic electrolyte and diffuses toward the cathode surface, where it is subsequently reduced to products such as methanol. Concurrently, OER occurs in the anode chamber, generating O_2 and H^+. The generated H^+ then migrates through the ion-exchange membrane or salt bridge to the cathode chamber, where it participates in the CO_2RR.

The advantages of the H-type cell lie in its simple structure and ease of operation, making it well suited for fundamental laboratory-scale research. However, its limitations include low CO_2 solubility in the electrolyte, poor mass transfer efficiency, and limited product selectivity.

The gas diffusion electrolyzer addresses the problem of low CO_2 solubility by delivering gaseous CO_2 directly to the electrode interface via a gas diffusion electrode (GDE) (Fig. 3(b)). The GDE consists of a porous conductive substrate, a gas diffusion layer, and a catalyst layer,

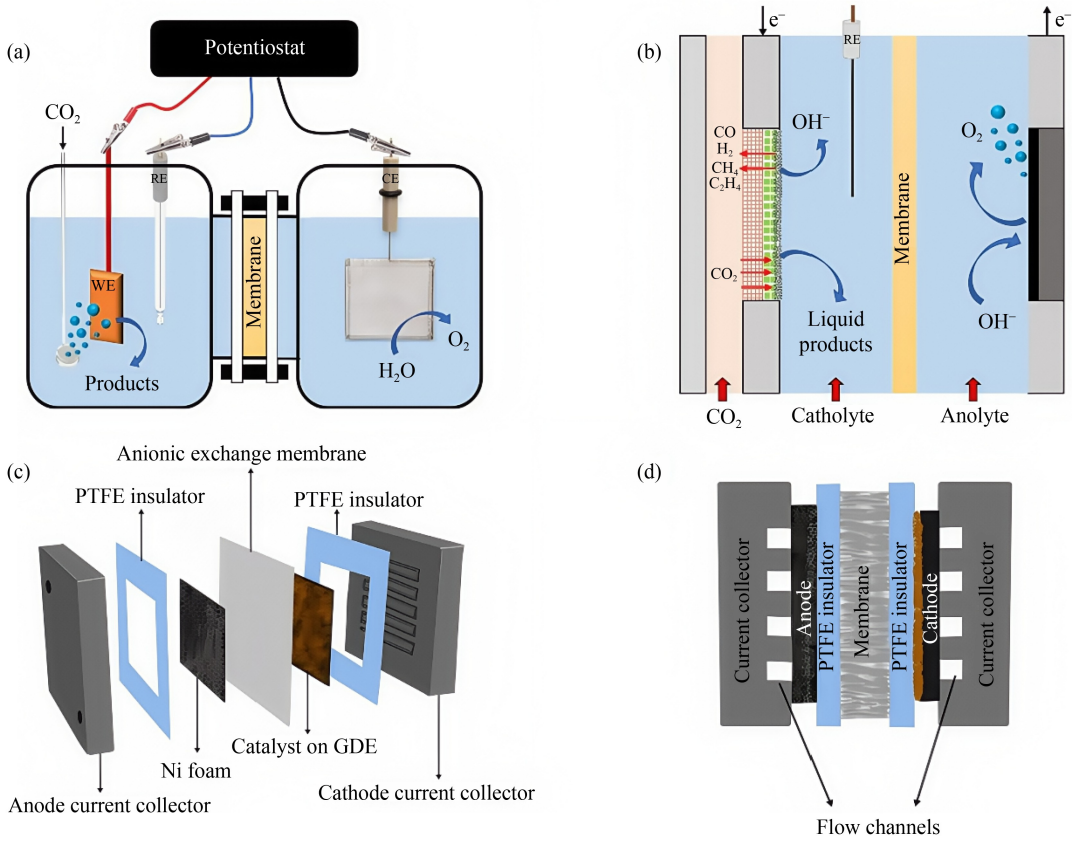

Fig. 3 Schematic diagrams illustrating different components and configurations of an electrochemical CO_2 reduction system. (a) Schematic diagram of a conventional H-type electrochemical cell; (b) schematic diagram of a basic gas-fed flow electrolyzer (reproduced with permission from Hernandez-Aldave and Andreoli [34], copyright 2020, MDPI); (c) schematic representation of a MEA; (d) cross-sectional view of an assembled MEA (reproduced with permission from Chandrashekar et al. [35], copyright 2021, Wiley).

forming an efficient three-phase (gas–liquid–solid) reaction interface [34]. During the CO_2RR process, gaseous CO_2 is directly transported through the porous structure of the GDE to the catalyst surface, where it subsequently reduced into products such as methanol. The anode chamber functions to the H-cell, where the OER occurs to produce H^+ ions. The generated H^+ then migrates through the membrane to the cathode, participating in the CO_2RR. Compared with the H-type cell, this configuration offers high CO_2 mass transfer efficiency and can achieve higher current densities. However, the electrode structure is more complex and expensive, and the reaction requires optimization of electrode hydrophobicity and stability to achieve selective production of target products.

MEAs integrate the cathode, anode, and proton exchange membranes (e.g., Nafion) into a compact electrochemical reactor (Figs. 3(c) and 3(d)) [35]. At the cathode, catalysts are usually loaded onto the electrode surface to catalyze CO_2RR. At the anode, the water oxidation reaction occurs, providing the H^+ required for the entire cycle. The proton exchange membrane facilitates H^+ transport while physically separating the cathode and anode compartments. During operation, humidified CO_2 is continuously fed into the cathode chamber. The GDE then delivers a high concentration of CO_2 to the cathode surface, where it is subsequently reduced to products such as methanol. Concurrently, water oxidation at the anode generates H^+, which migrates through the proton exchange membrane to the cathode to participate in the reduction reaction. This integrated configuration offers advantages of compactness and energy efficiency, making it suitable for large-scale applications and continuous operation. However, the high cost of membrane materials and their susceptibility to contamination remain challenges. Further in-depth studies into the interfacial properties and mass transfer between the catalyst and membrane are essential to enhance overall reaction efficiency.

In electrocatalytic systems, the formation of precipitates during cathodic reactions that readily adsorb onto electrode surfaces can significantly compromise system stability and catalytic efficiency. At elevated cathode potentials, cations such as potassium and sodium in the electrolyte readily combine with anions like carbonate and bicarbonate to form insoluble salts. These precipi-

tates adsorb onto the electrode surface, blocking the active sites of the catalyst and impeding mass transfer during the reaction. Consequently, optimizing the catalytic system is essential to suppress cathodic precipitation.

Currently, the industrial-scale implementation of electrocatalytic CO_2 reduction to methanol remains constrained by high costs and energy requirements. Similarly, photocatalytic CO_2 conversion faces scalability challenges due to low quantum efficiency and limited stability, although it has demonstrated promising progress toward industrialization. The cross-scale construction of photothermal co-catalytic systems offers valuable engineering paradigms for industrial applications such as methane reforming and water splitting [36]. Through optimization of reactor structure (e.g., tower concentrators and flat-plate membrane integrations) and system coupling, photothermal catalysis has achieved engineering demonstrations ranging from laboratory scale to installations exceeding hundred square meters. However, critical challenges persist in maintaining long-term stability and improving photothermal synergy efficiency requiring, both of which require further enhancement [37].

4 Recent progresses in electrocatalytic CO_2RR to methanol

4.1 Catalyst

With the continuous deepening of catalyst research, an increasing number of catalysts have become available for the electrocatalytic reduction of CO_2 to methanol. Based on the phase state of the catalyst and the reactants, these catalysts can be broadly classified into two categories: heterogeneous catalysts and homogeneous catalysts (Fig. 4) [38]. The following section outlines current research advances in various types of catalysts.

In general, Cu based catalysts remain the predominant choice for the electrocatalytic reduction of CO_2 to methanol. For the preparation of C_{2+} products, non-copper catalysts (such as silver, tin, and molecular catalysts) and other carbon-based materials employ distinct enrichment strategies. Non-copper catalysts such as Ag and Sn are primarily employed to produce C_1 products like carbon monoxide (CO) and formic acid (HCOOH). These catalysts can be coupled with Cu through interfacial engineering or tandem catalysis strategies to achieve surface enrichment of CO, thereby altering the reaction pathway [39].

Molecular catalysts enable precise control over their structure and environment, utilizing confinement effects to enrich carbon sources or reaction intermediates [40]. Carbon-based materials, characterized by high specific surface area and excellent conductivity, can be engineered through nitrogen doping or vacancy introduction to modulate their electronic structure. This modification enhances *CO adsorption, thereby promoting the kinetics of CO_2 reduction [41].

4.1.1 Heterogeneous catalysts

Heterogeneous catalysts are the most widely used in CO_2RR, and significant progress has been made in their application for the electrocatalytic reduction of CO_2 to methanol. As summarized in Table 1, the most extensively studied catalyst types include Cu-based catalysts, noble metal catalysts, molecular catalysts, and enzyme catalysts. Representative examples of each type will be discussed in detail below.

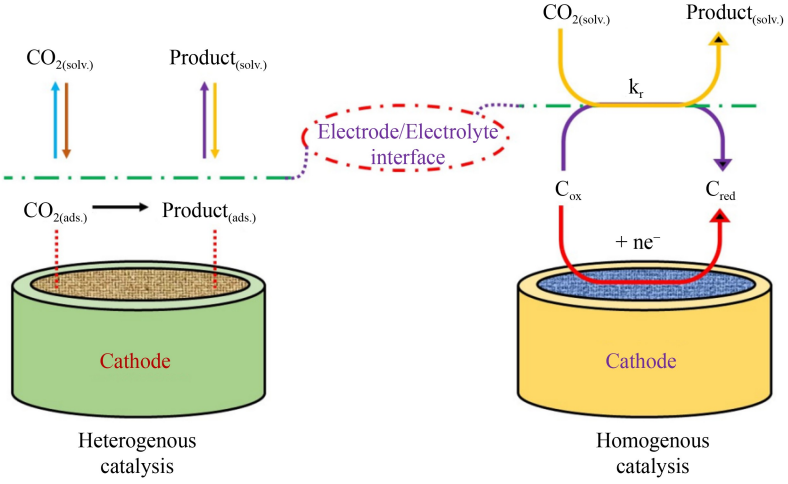

Fig. 4 Schematic diagram for homogeneous and heterogeneous catalysis (reproduced with permission from Al-Rowaili et al. [42], copyright 2018, ACS Publishers).

Table 1 Selected examples of methanol production by electrocatalytic CO_2RR over heterogeneous catalysts

Catalyst	Electrolyte	Electrolytic cell	Potential	Mathanol FE/%	Current density/ ($mA \cdot cm^{-2}$)	Partial current density/ ($mA \cdot cm^{-2}$)	Ref.
Cu_2O/CuO	0.5 mol/L $KHCO_3$ + 10 mmol/L pyridine + HCl (pH = 5)	H-cell	−1.3 V vs. Ag/Ag+	6.46	–	–	Murthy et al. [46]
Cu_3P@C	0.3 mol/L $KHCO_3$	H-cell	−0.36 V vs. RHE	59.2	–	–	Yu et al. [49]
	1.0 mol/L KOH	Flow cell	−0.36 V vs. RHE	61.2	–	–	
$Pd_{1.80\%}/MnO_2$	1.0 mol/L KOH	Flow cell	−0.6 V vs. RHE	80.9 ± 1.5	243.5 ± 4.3	197 ± 6.7	Zhu et al. [56]
		MEA Electrolyzer	3.2 V cell voltage	77.6 ± 1.3	250.8 ± 4.3	194.6 ± 5.1	
CoPc/CNT/C	0.1 mol/L bicarbonate solution	H-cell	< −0.7 V vs. RHE	<30	3.8 ± 0.5	1.14 ± 0.15	Yu et al. [72]
CoPc	0.5 mol/L $KHCO_3$	–	–	19.5	–	–	Boutin et al. [71]
CoPc/CNT	0.1 mol/L $KHCO_3$	–	−0.94 V vs. RHE	44	−23.69	−10.42	Rooney et al. [74]
CoPc-NH_2/CNT	0.1 mol/L $KHCO_3$	–	−1.0 V vs. RHE	32 (1 h) 2 (12 h)	10.2 (1 h) 8.9 (12 h)	3.26 (1 h) 1.78 (12 h)	Wu et al. [73]
CoPc-NH_2/CNT	0.3 mol/L $KHCO_3$	Flow cell	–	43	–	–	Cheon et al. [76]
CoPc/MWCNT	0.1 mol/L $KHCO_3$	Flow cell	−1.2 V vs. RHE	36±3	0.25	0.09	Chan et al. [79]
ball-milling-CoTAPc/CNT	0.5 mol/L $KHCO_3$	H-cell	−1.3 V vs. RHE	10.8	6.5	0.7	Guo et al. [80]
CoTmTPyPz/CNT/CP	0.5 mol/L $KHCO_3$	–	−1.0 V vs. RHE	15	–	–	Zhang et al. [81]
(CoPc-NH_2 + NiPc-OCH_3)/CNT	0.1 mol/L $KHCO_3$	H-cell	−0.98 V vs. RHE	43.4	13.7	5.94	Li et al. [82]
	0.3 mol/L KHCO3	Flow cell	−1.38 V vs. RHE	50	150	75	
CoPc/CNT	0.1 mol/L $KHCO_3$	H-cell	−1.0 V vs. RHE	26	–	–	Zhang et al. [85]
Sn_1/V_o-CuO-90	[Bmim]BF_4/H_2O (mole ratio 1:3)	H-cell	−2.0 V vs. Ag/Ag^+	88.6	67.0	59.36	Guo et al. [117]
Cu_{58}-I NC	0.1 mol/L $KHCO_3$	H-cell	−0.7 V vs. RHE	≈ 54	–	–	Biswas et al. [143]
$Mn_{4.8\%}$-VS_2	1.0 mol/L KOH	Flow cell	−0.6 V vs. RHE	72.5 ± 1.1	74.3 ± 1.1	53.8 ± 1.1	Wang et al. [144]
CuSAs/TCNFs	0.1 mol/L $KHCO_3$	–	−0.9 V vs. RHE	44	−93	−40.92	Yang et al. [145]
PO-5 nm	0.1 mol/dm^3 $NaHCO_3$	–	−0.90 V vs. SCE	71.4	4	2.85	Huang et al. [146]
Co/SL-NG			−1.0 V vs. SCE	23.2	10	2.32	
Pt_xZn/C ($1 < x < 3$)	0.1 mol/L $NaHCO_3$ (pH = 6.8)	–	−0.9 V vs. RHE	81.4	–	–	Payra et al. [147]
Mo_2C/N-CNT	0.1 mol/L $KHCO_3$	–	−1.1 V vs. SHE	80.4	–	–	Zhang et al. [148]
Cu_2NCN	0.5 mol/L $KHCO_3$	H-cell	−0.67 V vs. RHE	64	−5.1 (−0.8 V)	−3.26 (−0.8 V)	Kong et al. [149]
		MEA-based electrolyser	3.4 Vcell voltage	70	−92.3	−64.61	
$CuGa_2$	0.5 mol/L $KHCO_3$	H-cell	−0.3 V vs. RHE	77.26	–	–	Bagchi et al. [150]
Cu_9Ga_4	0.5 mol/L $KHCO_3$	H-cell	−0.1 V vs. RHE	37.75	–	–	
Cu-Y/CS:PVA MCE	1 mol/L KOH pH=10	–	−0.18 V vs. RHE	68.05	129	87.78	Marcos-Madrazo et al. [151]

4.1.1.1 Cu-based catalysts

Among the many catalysts for the electrocatalytic reduction of CO_2 to methanol, Cu-based catalysts are the most extensively studied. This is because Cu exhibits a moderate adsorption capacity for both CO_2 and reduction intermediates, enabling the production of variety of CO_2 reduction products [42]. This property not only effectively adsorbs CO_2 molecules, enriching them on the surface of the catalyst to enhance reaction probability, but also allows reduction products to desorb at the appropriate time. This prevents product over-adsorption and the consequent occupation of active sites, which will otherwise impede subsequent reaction steps.

Cu commonly exposes three crystal facets: Cu(100), Cu(110), Cu(111) [43]. These facets exhibit distinct catalytic and adsorption behaviors (Figs. 5(a) and 5(b)). The Cu(100) lattice structure facilitates CO_2 bending activation and promotes efficient *CO dimerization, favoring C–C bond formation and C_2 product generation. In contrast, the grooved Cu(110) surface exhibits strong *CO adsorption that impedes intermediate conversion and induces high surface coverage. The Cu(111) facet, characterized by a hexagonal close-packed compact structure, shows weak adsorption strength for CO_2 and *CO but moderate adsorption for key reaction intermediates

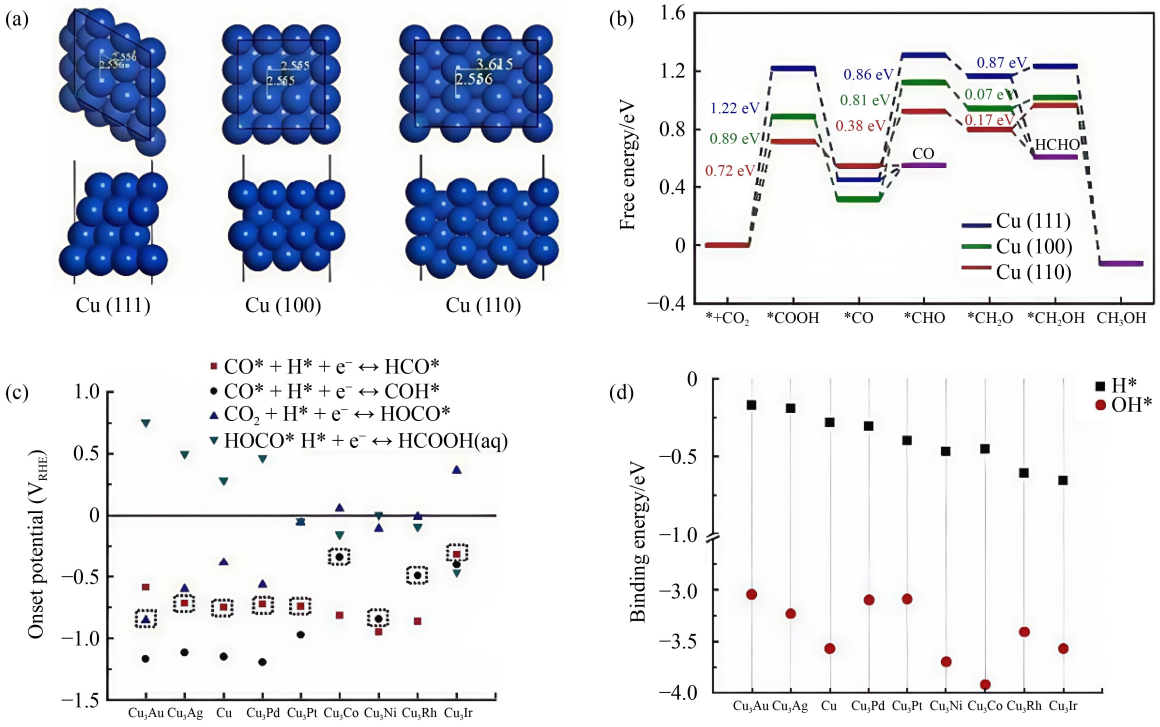

Fig. 5 Computational insights into the catalytic behavior of copper-based surfaces for CO_2 reduction.

(a) Top view and side view of the optimized structures of Cu(111), Cu(100), and Cu (110), respectively; (b) free energy diagram of CO_2RR to CO, HCHO, and CH_3OH over Cu (111), Cu (100), and Cu (110), respectively (reproduced with permission from Xue et al. [44], copyright 2023, MDPI Publishers); (c) onset potentials of the CO_2, HOCO*, and CO* protonation step (The dot squares indicate the calculated limiting potential step on $Cu_3X(211)$ surfaces.); (d) OH* and H* binding energies on $Cu_3X(211)$ surfaces (reproduced with permission from Hirunsit et al. [48] copyright 2015, ACS Publishers).

such as *CHO and *CH_2O. Due to the high coordination number of surface atoms, Cu(111) inhibits C–C coupling while promoting stepwise hydrogenation toward methanol. This pathway initiates with CO_2 activation to form *COOH, followed by reduction to *CO. Sequential hydrogenation proceeds through *CHO, *CH_2O, and *CH_3O intermediates before final protonation yields CH_3OH.

In a representative study, Gao et al. employed isotope labeling techniques to investigate the electrocatalytic activity of two specific sites on Cu. They identified Cu_{CO_2} as corresponding to the Cu(111) site and Cu_{CO} as a defective site. Both sites facilitate CO_2RR, with the Cu_{CO_2} site primarily promoting CO_2RR to CO, and the Cu_{CO} site favoring further reduction of CO to C_{2+} products. Notably, the activity for CO adsorption leading to C_{2+} product formation at the Cu_{CO} site was found to be at least 6-fold higher than that at the Cu_{CO_2} site [44].

Cu-based catalysts can be optimized to promote CO_2RR toward methanol by tuning their oxidation states and compositions, which in turn alters their electronic structures and surface properties. The overall methanol yield depends on factors such as the density of active sites, metal-support interactions and the functional additives [45]. Notably, adjusting the oxidation state of Cu has been shown to promote methanol formation. Leveraging the properties of Cu oxides, Roy et al. [47] fabricated Cu_2O/CuO electrocatalysts on porous nickel foam via electrodeposition followed by annealing. Catalysts annealed in air at 300 °C for 2 h exhibited optimal performance, achieving a current density of 46 mA/cm^2, although the Faradaic efficiency (FE) for methanol remained low at approximately 6% [46]. This enhanced CO_2RR activity was attributed to improved charge transfer between the electrode and catalyst, facilitated by the growth of the mixed Cu phase on the nickel foam. During CO_2RR, adsorbed CO molecules on the Cu_2O/CuO surface play a critical role in forming *HCO intermediates, which undergo PCET to generate *CH_3O adsorbate, ultimately yielding methanol.

Another strategy to enhance methanol production involves forming Cu alloys. By tuning the alloy composition, the CO_2RR pathway can be modulated. To explore this, Roy et al. [47] conducted density functional theory (DFT) calculations based on the standard hydrogen electrode model to investigate CO_2RR on Cu-based alloys (Cu_3X). Figure 5(c) compares the onset potentials for CO_2RR on pure Cu and eight Cu-based alloy surfaces. These results, combined with step potentials for CO_2RR

to formic acid, indicate that formic acid formation is more favorable on Cu_3Pt, Cu_3Ni, Cu_3Co and Cu_3Rh surfaces. However, competing HER and the excessive accumulation of OH* species, leading to OH* poisoning, negatively impact catalyst activity [48]. Analysis of OH* and H* binding energies on these surfaces (Fig. 5(d)) reveals that methanol formation is more favorable on Cu_3Pd and Cu_3Pt surfaces. Crucially, methanol selectivity depends on creating favorable conditions for the formation of the CH_2OH* intermediate, which occurs when protonation preferentially happens at the C atom rather than the O atom.

In addition to tuning the oxidation state and composition, carbon cladding also significantly influences the properties of Cu-based catalysts and offers multiple advantages. The carbon layer prevents Cu particles from sintering and agglomerating under high temperatures or reactive conditions, thereby stabilizing the catalytic structure. Additionally, the carbon layer facilitates electron transport due to its excellent electrical conductivity, significantly enhancing catalytic activity and efficiency. Furthermore, the surface properties of the catalyst can also be flexibly modulated through carbon coating, enabling Cu-based catalysts to operate effectively in more complex reaction environments.

In a recent study, Yu et al. [49] synthesized carbon-coated Cu materials and observed the formation of key intermediates (*COOH and *OCHO) during CO_2RR. They demonstrated that the surface charge of the catalysts modulates the reaction intermediates, leading to different reaction pathways (Fig. 6(a)) [50]. As illustrated in Fig. 6(b), catalysts with different electron densities yield different products via these pathways. Specifically, Cu_2Se and $Cu_{1.8}S$ catalysts with lower electron densities on the carbon-coated surfaces predominantly generate formate, while Cu_3P catalysts with higher electron

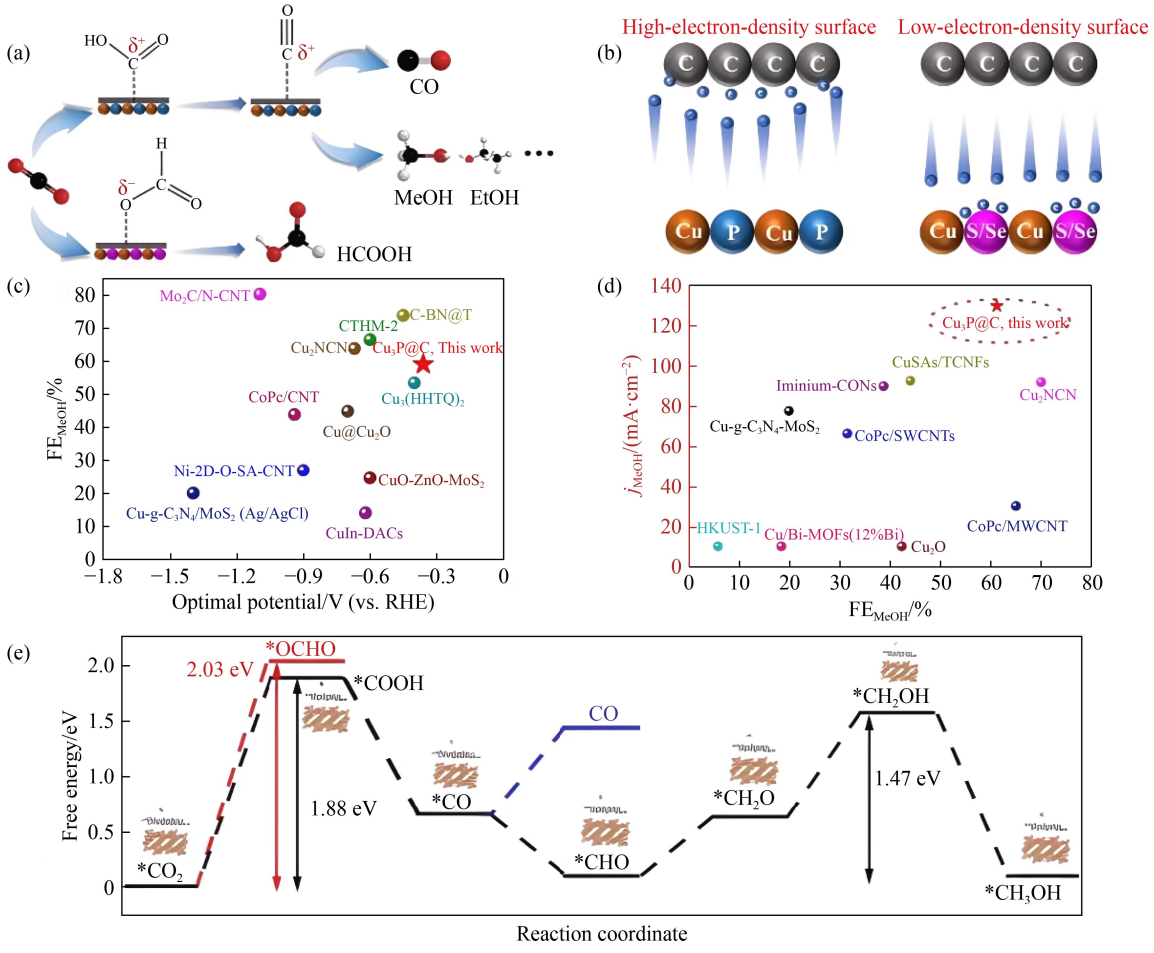

Fig. 6 Schematic illustration and performance analysis of catalysts for CO_2 electroreduction.

(a) Reaction pathways of different intermediates on electrocatalyst surfaces; (b) schematic illustration of electron transfer between Cu compounds and the carbon layer; (c) comparison of the CO_2RR performances with the state-of-the-art non-noble metal electrocatalysts in a H-cell; (d) comparison of the performance of Cu_3P@C in a flow cell setup with other state-of-the-art electrocatalysts. (e) energy level diagram of Cu_3P@C for CO_2 reduction to methanol (reproduced with permission from Yu et al. [49], copyright 2024, ACS Publishers).

densities on the carbon-coated surfaces favor methanol production. The Cu_3P catalysts demonstrated high methanol selectivity in both H-type cell and the flow cell systems. At −0.36 V vs. RHE, the Cu_3P@C catalyst achieved a methanol FE of 59.2% in the H-type cell. When operated in a flow cell with 1 mol/L KOH electrolyte, the FE of methanol reached 61.2% at 0.76 V vs. RHE, with a partial current density of 130 mA/cm^2, outperforming many reported electrocatalysts for the methanol production (Figs. 6(c) and 6(d)). The energy level diagram in Fig. 6(e) further confirms that the carbon-coated Cu_3P surface thermodynamically favors the methanol formation pathway.

In summary, copper-based catalysts remain central to the electrocatalytic conversion of CO_2 to methanol by virtue of advanced optimization strategies such as oxidation state tuning, alloying, and carbon coating. Nonetheless, maintaining catalytic efficiency over prolonged operation continues to be a critical challenge for their practical application.

4.1.1.2 Noble metal catalysts

In the electrocatalytic CO_2RR for methanol production, noble metal catalysts demonstrate unique advantages by significantly enhancing methanol selectivity. Noble metals such as platinum (Pt), Ruthenium (Ru), rhodium (Rh), and palladium (Pd) are commonly employed as primary active components due to their excellent electronic conductivity and distinctive electronic structures. These properties provide abundant active sites for CO_2RR, reducing the activation energy of the reaction, thereby exhibiting high catalytic activity.

The design noble metal catalysts for electrocatalytic CO_2RR can be inspired by principles from thermocatalytic CO_2 hydrogenation. In pioneering work, Kothandaraman et al. [51] demonstrated the use of polyamine-supported homogeneous Ru catalysts to convert atmospheric CO_2 into methanol, achieving a remarkable methanol conversion rate of 79%.

This achievement represents a significant milestone toward realization of a future “methanol economy”. More recently, Chen et al. [52] identified the formate pathway as the optimal route for CO_2 hydrogenation to methanol on Rh cluster-loaded In_2O_3 (111) surface among three proposed pathways. In this mechanism, CO_2 first adsorbs onto the catalyst surface and reacts with active hydrogen atoms to form HCOO* intermediate, which then undergoes sequential hydrogenation steps to produce methanol. The maximum conversion efficiency observed for this pathway reached 3.02×10^{-5} s^{-1}. This high methanol conversion efficiency is attributed to Rh clusters promoting both CO_2 adsorption and hydrogen dissociation, thereby greatly enhancing catalyst performance. In addition, studies on thermocatalytic CO_2 hydrogenation to methanol utilizing other noble metals such as Pd and Pt have also yielded promising results [53,54].

Findings from thermocatalytic CO_2 hydrogenation reveal that noble metal catalysts such as Ru and Rh demonstrate high stability and catalytic activity for the CO_2RR to methanol. Their high efficiency in converting CO_2 to methanol is mainly attributed to their unique electronic structures and catalytically active sites. Specifically, the electron cloud distribution around Ru atoms enables effective adsorption and activation of CO_2 molecules, which reduces the activation energy of CO_2 and facilitates electron transfer, thereby accelerating methanol generation.

Building on this principle, Zhang et al. [55] designed a Pd/SnO_2 catalyst with a high CO_2 adsorption capacity. Their study revealed that the resulting Pd-O-Sn interface is particularly favorable for the reduction of CO* intermediates to methanol, providing a novel approach for enhancing the electrocatalytic CO_2RR to methanol via the strategic construction of metal oxide interfaces.

In a recent study, Zhu et al. [56] synthesized MnO_2 nanosheets via a hydrothermal method and subsequently deposited Pd nanoparticles onto MnO_2 nanosheets using solution-phase deposition, creating composite catalysts with varying Pd loadings (denoted as Pd NPs/MnO_2 NSs). The morphology of the $Pd_{1.80\%}/MnO_2$ catalyst is characterized and shown in Figs. 7(a)–7(e). Its CO_2RR performance was evaluated in both flow cell and a MEA electrolyzer. In the flow cell with a 1.0 mol/L KOH electrolyte, $Pd_{1.80\%}/MnO_2$ exhibited the highest CO_2RR catalytic activity among tested loadings, achieved a methanol FE of 80.9 ± 1.5% and a high partial current density of 243.5 ± 4.3 mA/cm^2 at −0.6 V vs. RHE (Figs. 7(f)–7(g)). In the MEA electrolyzer, the same catalyst achieved a methanol FE of 77.6 ± 1.3% at 3.2 V vs. RHE, with a methanol partial current density of 250.8 ± 4.3 mA/cm^2 and a full-cell energy efficiency of 29.1 ± 1.2%. This excellent catalytic performance is attributed to the Pd nanoparticles modulating the electronic structure of MnO_2 and inducing oxygen vacancies, which facilitate CO_2 activation and intermediate conversion to methanol (Fig. 7(h)). In addition, palladium doping has also shown excellent catalytic performance for CO_2 reduction to C_{2+} products [57].

In summary, ongoing exploration of noble metal catalysts has significantly advanced research in the electrocatalytic conversion of CO_2 to methanol, contributing substantially to resource conservation and environmental protection. However, challenges such as high production costs and susceptibility to environmental factors that degrade catalytic performance [58] limit the

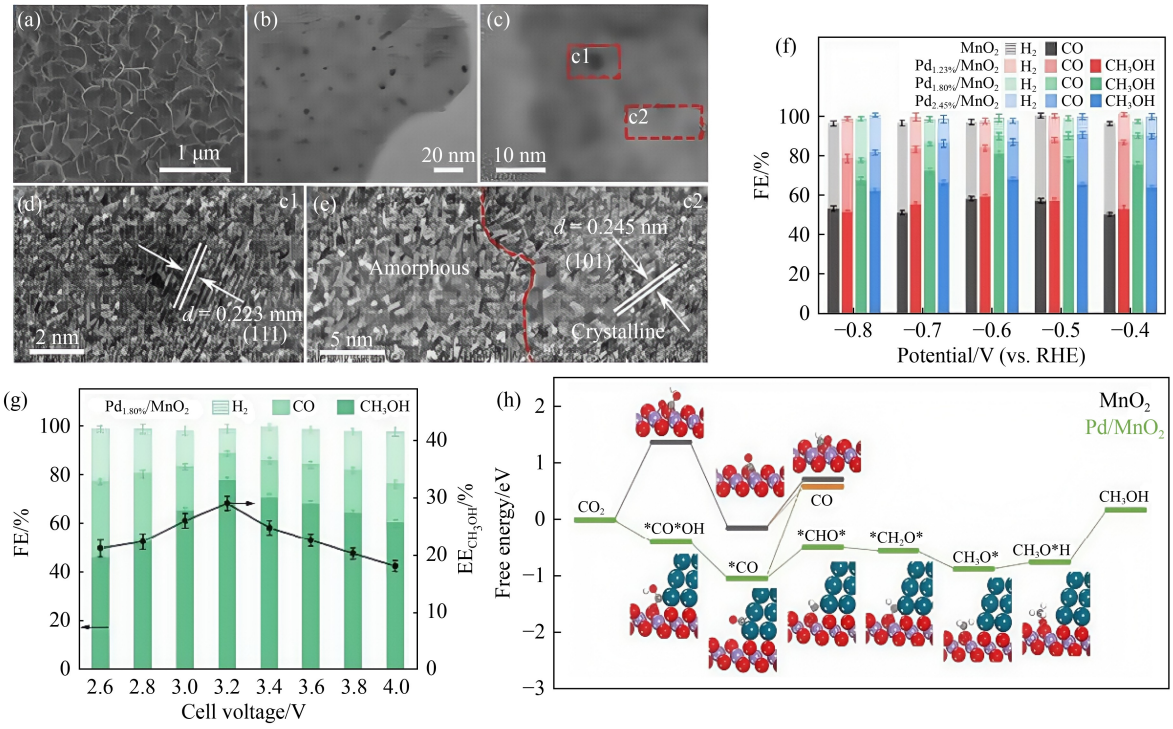

Fig. 7 Structural characterization and electrocatalytic performance of Pd-doped MnO_2 for CO_2 reduction.

(a) SEM image; (b) TEM image; (c–e) HRTEM images of $Pd_{1.80\%}/MnO_2$; (f) FEs of methanol, CO, and H_2 from −0.4 to −0.8 V with an interval of 0.1 V in flow cells; (g) FEs of methanol, CO, and H_2 and EE of methanol at different cell voltages in an MEA electrolyzer by coupling OER; (h) Gibbs free energy profiles for the reduction of CO_2 on MnO_2 (in black) and Pd/MnO_2 (in green) (Mn: purple; Pd: green; O: red; C: gray; H: white) (reproduced with permission from Zhu et al. [56], copyright 2023, ACS Publishers).

large-scale deployment of noble metal catalysts in the foreseeable future.

4.1.1.3 Molecular catalysts

Unlike heterogeneous catalysts, molecular catalysts provide distinct advantages in precise active site identification, reaction mechanism elucidation, and structural tunability [59,60]. Their well-defined active sites, typically metal centers coordinated to specific ligands, enable precise control over catalytic active units and a deeper mechanistic understanding. By tuning the electronic property and spatial resistance of the ligand, the electron density at metal centers can be finely adjusted to optimize reaction pathways. In addition, metal-centered engineering via substitution or modification allows targeted regulation of substrate and intermediates interactions, thereby lowering the energy barrier of rate-determining steps. Currently, molecular catalysts have demonstrated significant progress in diverse fields, including CO_2RR [61,62], alkane dehydrogenation [63], hydrogen preparation [64], and fuel cell research [65].

Metal-organic frameworks (MOFs) represent a promising class of molecular catalysts that have demonstrated highly efficient electrocatalytic activity for methanol production via CO_2RR [66,67]. For example, MOF-derived nickel nanoparticles have exhibited catalytic activity for CO_2 reduction over a wide potential window [68]. In a representative study, Albo et al. [69] loaded four MOFs, i.e., HKUST-1, CuAdeAce, CuDTA mesoporous metal-organic aerogel (MOA), and CuZnDTA MOA, onto a GDE. They observed that the MOF-modified GDE enhanced CO_2RR performance, producing liquid-phase products including methanol with significant efficiency. Among these, the HKUST-1-based electrode achieved a FE of 5.6% for CO_2-to-methanol conversion. Similarly, Zhao et al. [70] utilized a Cu/C-derived MOF electrode and achieved a remarkable methanol FE of 43.2% under optimal conditions.

The discovery and development of cobalt phthalocyanine (CoPc) and its derivatives represent significant progress in the electrocatalytic CO_2RR for methanol production. CoPc catalysts offer notable advantages such as simple preparation methods, relatively low catalyst loading, and the ability conversion of CO_2 to CO [71]. Notably, the subsequent reduction of CO to methanol under acidic conditions, especially in the presence of alkali metal cations, significantly enhances the overall

CO_2-to-methanol conversion rate [72].

In 2019, Wu et al. [73] first demonstrated the potential of CoPc by loading it onto carbon nanotubes (CoPc/CNT) and investigating its catalytic performance for methanol synthesis via CO_2RR. It was found that the reaction proceeds via a distinct domino mechanism with CO as a key intermediate. Remarkably, the CoPc/CNT catalyst achieved a FE for methanol exceeding 40% at 0.94 V versus RHE in a near neutral electrolyte.

Subsequent research highlighted the critical role of CoPc dispersion on the CNT support. Rooney et al. [74] showed, supported by mechanistic studies, that the molecular dispersion state of CoPc on the CNT surface is crucial for enabling rapid electron transfer to active sites and efficient multi-electron CO_2 reduction. Therefore, CoPc on CNTs typically exists in two distinct states: well-dispersed and aggregated. These configurations exhibit distinct structural and performance characteristics, with aggregated CoPc/CNT primarily producing CO, whereas the well-dispersed CoPc/CNT favors methanol formation [75].

Despite significant catalytic activity, CoPc/CNT catalysts suffer performance degradation over time due to the detrimental reduction of phthalocyanine ligands. This deactivation can be mitigated by introducing electron-donating amino substituents onto the phthalocyanine ring, yielding CoPc-NH_2/CNT catalysts with enhanced stability, activity, and selectivity for CO_2-to-methanol conversion [73]. Remarkably, CoPc-NH_2/CNT catalyst achieves a methanol FE of 32%, maintaining 28% FE after 12 h of operation. Further improvements were realized in a flow cell configuration, where a methanol FE of a 43% was reported [76]. Furthermore, CoPc-NH_2/CNT catalysts effectively convert carbon monoxide to methanol, achieving an 85% FE under optimized conditions with pH-independent behavior [77]. Notably, the *CO intermediates generated during CO_2 and CO reduction exhibit distinct adsorption structures, influencing their reaction pathways [78].

Beyond amino-functionalized derivatives, other cobalt-based molecular catalysts show promise for electrocatalytic CO_2-to-methanol conversion, including CoPc loaded onto multi-walled carbon nanotubes (CoPc/MWCNT), Co(II)2,9,16,23-tetrakis(amido)phthalocyanine(CoTAPc) composites, and tetramethylcobalt(II) tetrapyridylpyrazine (CoTmTPyPz) [79–81].

To further enhance methanol selectivity, Li et al. [82] recently designed a dual-site catalyst by co-loading nickel tetramethoxyphthalocyanine (NiPc-OCH_3) and CoPc-NH_2 onto multiwalled carbon nanotubes (MWCNTs). This dual-site system achieves a methanol FE of 50% with a partial current density of 150 mA/cm^2, significantly outperforming the single-site CoPc-NH_2/CNT catalyst. This enhancement is attributed to CO spillover from NiPc-OCH_3 sites to the methanol-active CoPc-NH_2 sites, which dramatically accelerates methanol production.

In another approach, Song et al. [83] synthesized a novel covalent organic nanosheet (CON) with an ultrathin layered structure (Fig. 8(a)) and increased Co active sites by utilizing the spatial site resistance from tert-butyl groups and electrostatic effects. Electrocatalytic testing showed that these iminium-CONs exhibit promising CO_2-to-methanol conversion efficiencies (Figs. 8(b) and 8(e)). Given the multi-step PCET mechanism involved, factors such as CO_2 partial pressure and mass transfer rates critically influence methanol yields [84–86].

In summary, molecular catalysts underscore the importance of precisely regulating the oxidation state and coordination environment of the metal centers for efficient CO_2-to-methanol conversion. This intrinsic tunability aligns closely with the fundamental properties of molecular catalysts, establishing them as a key focus for ongoing research.

4.1.1.4 Enzyme catalysts

Enzyme catalysts are distinguished by their high efficiency, enabling significantly faster reaction rates compared to conventional catalysts. This high catalytic performance stems from several inherent advantages of enzymes. First, each enzyme exhibits strict substrate specificity, allowing precise regulation of the reaction pathway. Second, enzyme possesses stereo-specificity, enabling precise control over the stereochemistry of the reaction to form desired enantiomeric products. Due to these characteristics, enzymes play crucial roles across diverse fields including biocatalysis [87], organic synthesis [88], fuel preparation [89,90], carbon dioxide fixation, and organic matter degradation [91,92]. However, a notable limitation is that enzyme-catalyzed reactions require strictly maintained mild conditions, particularly specific temperature and pH ranges.

The enzymatic reduction of CO_2 to methanol proceeds via a cascade of reactions involving key enzymes such as formate dehydrogenase (FateDH), formaldehyde dehydrogenase (FaldDH), and alcohol dehydrogenase (ADH). This process requires substantial coenzyme consumption to provide protons and energy, with nicotinamide adenine dinucleotide (NADH) serving as the predominant cofactor. To address NADH depletion, El-Zahab et al. innovatively incorporated glutamate dehydrogenase (GDH) into the system, enabling *in situ* NADH regeneration and significantly enhancing catalytic cycling efficiency (Fig. 9(a)) [93]. Currently, NADH regeneration has become a focal point of research, with major strategies including enzymatic, electrochemical, and

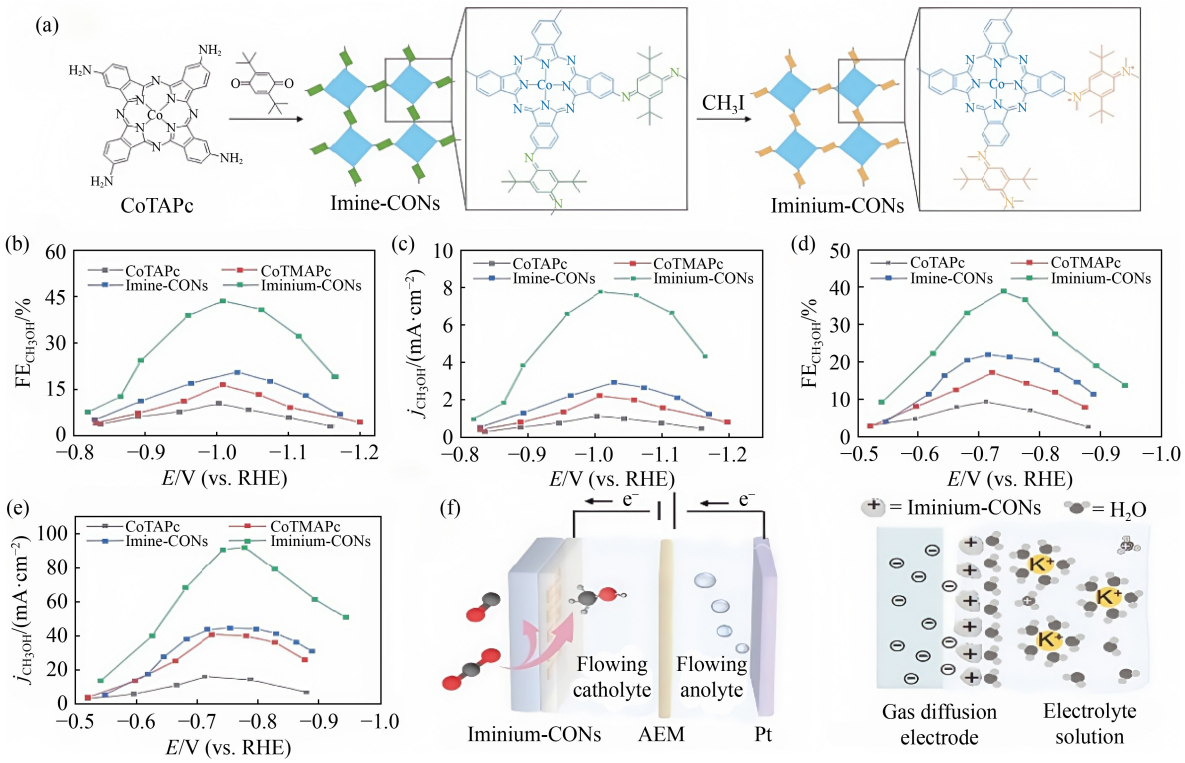

Fig. 8 Design and electrocatalytic performance of iminium-based covalent organic networks (Iminium-CONs) for CO_2 reduction. (a) Schematic illustration for the synthesis of iminium-CONs; (b) FE, and (c) partial current density toward methanol of CoTAPc, CoTMAPc, imine-CONs, and iminium-CONs in a H-cell; (d) FE, and (e) partial current density toward methanol of CoTAPc, CoTMAPc, imine-CONs, and iminium-CONs using mixed electrolyte of 0.2 mol/L KOH and 1.5 mol/L KCl in a flow cell; (f) schematic of electrochemical flow cell and interfacial ions on the catalyst surface (reproduced with permission from Chan et al. [79], copyright 2023, Wiley Publishers).

photochemical regeneration methods [94]. These regeneration strategies are detailed below.

Enzyme regeneration: Enzyme catalysts are increasingly utilized in bioelectrocatalytic systems for CO_2RR to methanol [95]. Schlager et al. [96] demonstrated this conversion by directly injecting electrons from the electrode into the immobilized enzyme, thereby avoiding the use of the coenzyme NADH (Fig. 9(b)). Their reactor employed carbon felt as the electrode and a mixed alginate-silicate gel matrix to immobilize formate dehydrogenase (FDH), formaldehyde dehydrogenase (FaldDH), and alcohol dehydrogenase (ADH). Electrolysis at −1.2 V (vs. Ag/AgCl) for 4 h produced approximately 0.15 ppm of methanol in a CO_2-saturated system, corresponding to a methanol FE of 10%. In some trials, methanol FE reached up to 30%. Control experiments confirmed no methanol production occurred under enzyme-free or N_2-saturated conditions, verifying the essential catalytic role of the enzyme. This study validates the feasibility of conducting CO_2 electrosynthesis without exogenous coenzymes.

Electrochemical regeneration: Zhang et al. [97] successfully constructed a novel bioelectrocatalytic system by embedding relevant enzymes into the metal-organic framework ZIF-8 and grafting a Rh complex (Cp*Rh(2,2-bipyridyl-5,5-dicarboxylic acid)Cl_2) onto the electrode for sustainable NADH regeneration. This approach overcame challenges of the poor CO_2 solubility in water and the high cost of NADH. Methanol production efficiency was significantly enhanced when the enzyme was immobilized within ZIF-8, reaching 0.320 mmol/L after 3 h, compared to much lower yields in conventional free-enzyme catalytic systems. Furthermore, the heterogeneous NADH regeneration enabled by the grafted Rh complex further boosted methanol production to 0.742 mmol/L, corresponding to a production rate of 822 μmol/(g·h), approximately 12 times higher than the conventional system. These results fully demonstrate the high efficiency and stability of this novel catalytic approach.

Photochemical regeneration: In addition to enzyme regeneration and electrochemical regeneration, photochemical regeneration is another effective method for NADH recovery. Ma et al. [98] designed a photoelectrocatalytic

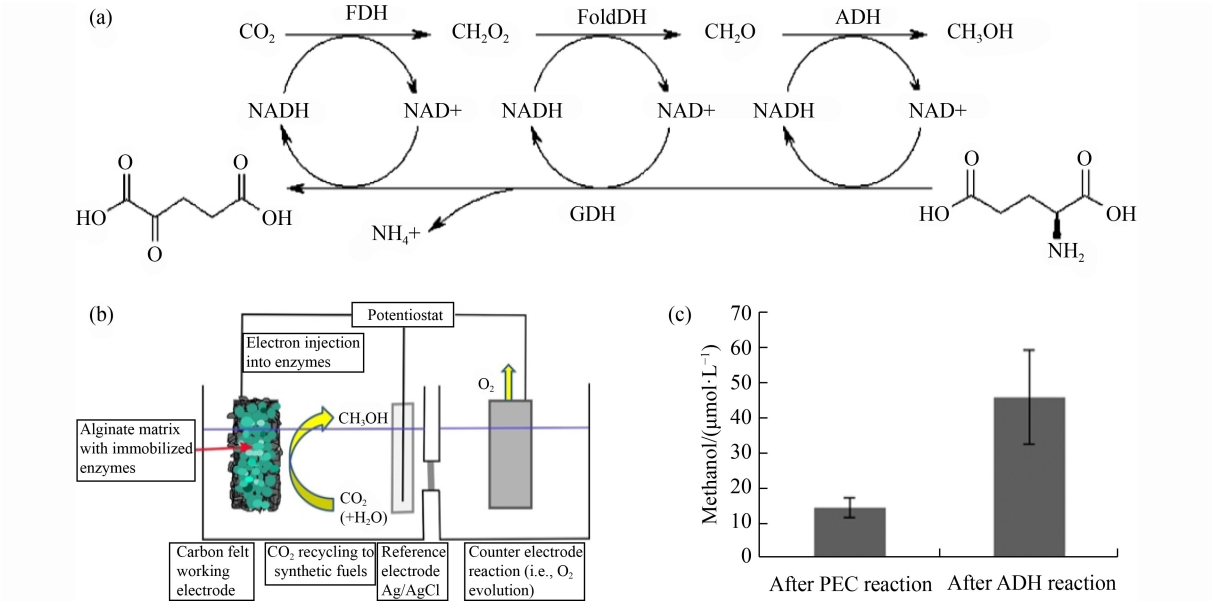

Fig. 9 Enzymatic and photoelectrochemical cascade system for CO_2 reduction to methanol.

(a) Chemical route of enzymatic synthesis of methanol from CO_2 with *in situ* regeneration of NADH (reproduced with permission from El-Zahab et al. [93], copyright 2007, Wiley); (b) representation of the electrochemical CO_2 reduction using enzymes (Electrons are injected directly into the enzymes, which are immobilized in an alginate-silicate hybrid gel (green) on a carbon-felt working electrode.) (reproduced with permission from Schlager et al. [96], copyright 2016, Wiley); (c) comparison of methanol production from PEC reaction before and after addition of ADH (Error bars indicate one standard error from five replicate experiments) (reproduced with permission from Ma et al. [98], copyright 2016, ACS Publishers).

system combining alcohol dehydrogenase (ADH) from brewer's yeast (Saccharomyces cerevisiae) with the CO_2 reduction products generated by a photocatalytic cell (PEC). In this system, ADH reduced formaldehyde in solution to extremely low micromolar concentrations. The addition of ADH to PEC products increased methanol yield rapidly by 3 to 4 times, primarily attributed to the absence of reverse reactions. This study highlights the powerful potential of combining biocatalysts with synthetic photosystems to ultimately improve the efficiency of producing liquid fuels from carbon dioxide and water (Fig. 9 (c)).

In summary, the high efficiency and specificity of enzymes have drawn significant attention in catalysis. However, the stringent operational conditions required by enzymes limit their broader application in electrocatalytic CO_2 reduction. With advances in scientific techniques and instrumentation, research progress in enzyme catalysts continues to accelerate, promising new breakthroughs in the near future.

4.1.2 Homogeneous catalysts

Compared to heterogeneous catalysts, homogeneous catalysts are typically molecules or ions species uniformly dispersed within the reaction medium. This molecular-level dispersion maximizes catalyst-reactant contact and dispersion, thereby lowering reaction activation energy barriers and enhancing overall reaction rates. To date, homogeneous catalysts have played an important role in electrocatalytic CO_2RR, particularly for methanol production [99]. Their ability to facilitate efficient electrons transfer between electrodes and CO_2 molecules promotes both activation and subsequent reduction of CO_2, thereby improving reaction efficiency and methanol yield.

Pyridine and pyridazine are representative homogeneous catalysts widely studied for electrocatalytic CO_2RR to methanol. Protonated pyridine (pyridinium) notably promotes CO_2 conversion to methanol and has been studied extensively in both photocatalytic and electrocatalytic systems [100]. As early as 1993, Seshadri et al. [101] demonstrated that pyridinium ions enabled efficient CO_2RR to methanol, achieving approximately 30% FE at palladium hydride electrodes despite competitive hydrogen evolution reactions. This system operates effectively at low overpotentials, highlighting its practical advantage. Subsequent mechanistic studies established a general reaction pathway for pyridinium-catalyzed CO_2 reduction to methanol (Fig. 10(a)) [102]. Interestingly, substituting pyridine with 4-tert-butylpyridine significantly reduced methanol yield and eliminated formic acid production.

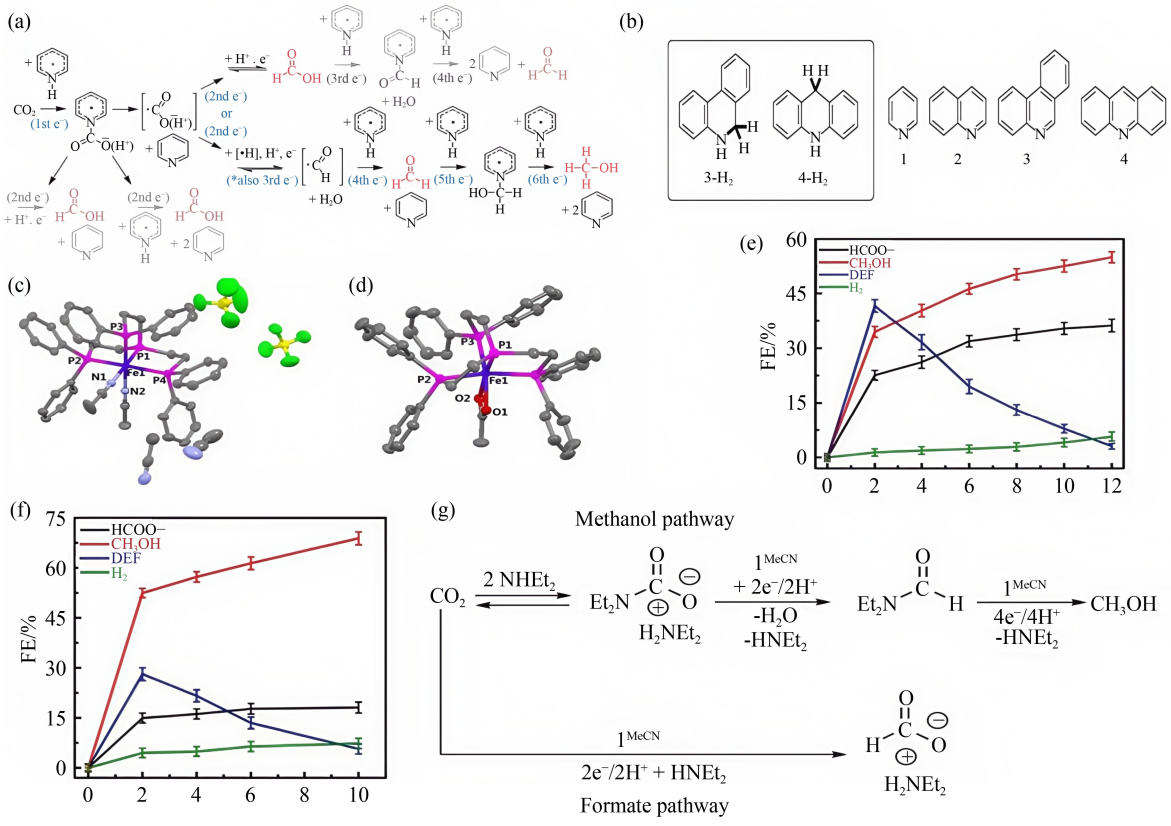

Fig. 10 Electrocatalytic CO_2 reduction to formate and methanol using cobalt phthalocyanine complexes with varying ligands.

(a) Overall proposed mechanism for the pyridinium-catalyzed reduction of CO_2 to the various products of formic acid, formaldehyde, and methanol (reproduced with permission from Barton Cole et al. [102], copyright 2010, ACS Publishers); (b) structures of DHPs and related ANHs studied as additives (reproduced with permission from Giesbrecht and Herbert [105], copyright 2017, ACS Publishers); (c) crystal structure of 1^{MeCN}; (d) crystal structure of 1^{OAc}. CPEs with added amine; (e) product distribution over time under CO_2; (f) product distribution over time under Ar, by adding CO_2 first, and then removing CO_2 by Ar purging; (g) proposed pathways for electrochemical reduction of CO_2 by 1^{MeCN} (reproduced with permission from Bi et al. [108], copyright 2019, Wiley).

This reduction is attributed to diminished catalyst charge-transfer capacity and energy-supply efficiency of the modified catalyst.

Portenkirchner et al. [103] further compared the CO_2RR performance of protonated pyridine and pyridazine at a Pt electrode, reporting methanol FEs of 14% ± 1.5% and 3.6% ± 0.5%, respectively. In addition, Rybchenko et al. [104] investigated pyridine-mediated CO_2RR to methanol conversion at elevated CO_2 pressure (55 bar), achieving up to 10% methanol FE. However, methanol concentration plateaued despite increased charge passed, suggesting limitations in sustained production. Cyclic voltammetry (CV) analysis showed that hydrogen precipitation dominated the electrode reaction and that CO_2 reduction to methanol was a transient process, decoupled from continuous electrode charge transfer.

Beyond these established systems, recent research has explored novel homogeneous catalysts for electrocatalytic CO_2RR to methanol. Giesbrecht et al. [105] investigated the electrochemical reduction of dihydropyridines such as 1, 2-dihydrophenanthridine and 9, 10-dihydroacridine, confirming that these species can convert CO_2 to methanol, with the electroreduction mechanism exhibiting strong electrode-surface dependence (Fig. 10(b)). In recent years, 6, 7-dimethyl-4-hydroxy-2-mercapto pteridine (PTE) has attracted attention for this application [106,107]. However, these studies reported unsuccessful CO_2 reduction to methanol under tested conditions, indicating limited catalytic efficacy for PTE in this reaction.

Bi et al. [108] investigated an iron complex, $[Fe(PP_3)(MeCN)_2](BF_4)_2$, featuring a tetradentate phosphine ligand a homogeneous catalyst for electrocatalytic CO_2RR in acetonitrile (Figs. 10(c) and 10(d)). In the absence of amine additives, this iron complex selectively reduced CO_2 to formate with a high FE of 97.3%. Remarkably, introducing diethylamine as a co-catalyst shifted product selectivity toward methanol (Fig. 10(e)), achieving a methanol FE of 68.5% under optimized conditions (Fig. 10(f)). Mechanistic studies revealed that

diethylamine first reacts with CO_2 to form a carbamate intermediate, which is subsequently reduced by $[Fe(PP_3)](BF_4)_2$ through sequential steps to formamide and ultimately methanol (Fig. 10(g)). This study highlights a novel cooperative catalytic strategy leveraging amine additives for selective CO_2-to-methanol conversion.

In summary, different catalysts have been employed for the electrocatalytic CO_2 reduction to methanol, employing various enrichment strategies to enhance CO_2 adsorption and intermediate stabilization, as summarized in Table 2. For instance, Cu-based catalysts such as Cu_3P@C utilize electronic modulation and porous structures to improve CO_2 uptake and maintain a stable current density with a FE of approximately 60% for methanol over 24 h. Noble metal catalysts like $Pd_{1.80\%}/MnO_2$ introduce oxygen vacancies and specific atomic configurations to enrich CO_2 and stabilize intermediates, showing minimal activity loss over 60 h. Molecular catalysts such as CoPc-NH_2/CNT utilize *in situ* CO generation to activate deep reaction sites, though a gradual decline in FE of MeOH is observed within 100 h. Enzyme catalysts leverage encapsulation in porous frameworks like ZIF-8 for synergistic CO_2 and cofactor enrichment, significantly improving long-term stability compared with free enzymes. Homogeneous catalysts including $Fe(PP_3)(MeCN)_2$ employ amine additives to form carbamate intermediates, enabling stable current and increased methanol FE over 12 h. Collectively, these approaches contribute to enhancing both the efficiency and durability of methanol production from CO_2.

4.2 Electrolyte assisted CO_2RR to methanol

Using complementary strategies can significantly improve the electrochemical properties of materials [109]. Among these, electrolytes are essential components in electrochemical systems, serving as the reaction medium and profoundly influencing reactant distribution, mass transport, and electrode surface processes [110]. In the electrocatalytic CO_2RR system, selecting an appropriate electrolyte can regulate reaction pathways and product distribution by enhancing CO_2 solubility, thereby improving reactant-catalyst contact and overall catalytic efficiency.

Current research employs diverse electrolytes, including aqueous solutions, organic solvents, and ionic liquids (ILs), for electrocatalytic CO_2RR [111,112]. Among these, IL-based electrolytes have garnered particular attention due to their exceptional CO_2 solubility and high ionic conductivity, making them promising candidates for efficient electrocatalytic CO_2 conversion [113].

In 2011, Rosen et al. [114] reported a breakthrough in IL electrolytes for CO_2RR by demonstrating that 1-ethyl-3-methylimidazolium tetrafluoroborate ([Emim]BF_4) significantly reduces the energy barriers for CO_2 reduction intermediates (Fig. 11(a)). Since then, ILs have been widely applied in electrocatalytic CO_2RR to methanol with notable success.

For example, Sun et al. [115] developed a Mo-Bi bimetallic chalcogenide catalyst (Mo-Bi BMC), where Bi promotes CO_2-to-CO conversion while Mo generates H_2 for subsequent reactions, resulting in synergistic catalytic enhancement. Crucially, this system achieved a methanol FE of 71.2% in a 1-butyl-3-methylimidazolium tetrafluoroborate [Bmim]BF_4/acetonitrile electrolyte, substantially outperforming conventional electrolytes.

Similarly, Lu et al. [116] systematically studied Pd–Cu aerogel electrocatalysts, identifying $Pd_{83}Cu_{17}$ as the optimal electrocatalyst. When using an aqueous

Table 2 Enrichment strategies and durability of exemplary catalyst materials

Catalyst category	Example materials	Enrichment strategy	Durability testing	Ref.
Cu-based catalysts	Cu_3P@C	Modulating the electronic states of the carbon layer, reduces H^+ adsorption while enhancing CO_2 adsorption. The formation of a porous structure increases the catalyst surface area available for CO_2 contact.	Under specified conditions, after 24 h of testing in H-cells and flow-through cells, the current density remained relatively stable, with methanol FE of approximately 60%	Yu et al. [49]
Noble metal catalysts	$Pd_{1.80\%}/MnO_2$	Pd-induced MnO_2 oxygen vacancies adsorb CO_2, enhancing surface CO_2 concentration; the 'C-Pd-O-Mn' configuration effectively prevents desorption of intermediates	Under specified conditions in the flow cell for 60 h, the current density stabilized at –300 to –303 mA/cm^2. The methanol FE decreased slightly from an initial 80.9% to 78.0%	Zhu et al. [56]
Molecular catalysts	CoPc-NH_2/CNT	Using CO_2 as feedstock, CO is generated and enriched *in situ* within the catalyst layer. This *in situ* CO activates deep-seated active sites to promote methanol formation	At total current densities exceeding 200 mA/cm^2, the methanol FE decreased from 43% to 35% within 100 h	Cheon et al. [76]
Enzyme catalysts	FDH, FaldDH, ADH	ZIF-8 achieves CO_2 enrichment through hydrogen bonding and its porous structure, synergistically facilitating the accumulation of the coenzyme NADH in conjunction with Rh complexes	A 20-day stability study demonstrated that the residual activity of enzymes encapsulated within ZIF-8 reached 51%, whereas that of free enzymes was only 25%	Zhang et al. [97]
Homogeneous catalysts	$Fe(PP_3)(MeCN)_2$	Diethylamine can be enriched in acetonitrile electrolyte to form carbamate compounds. Subsequently, when the resulting DEF is reduced to methanol, diethylamine is released	Under 12 h of constant-potential hydrolysis, the methanol FE gradually increased to 55%, with the current density remaining stable and showing no significant decay	Wang et al. [108]

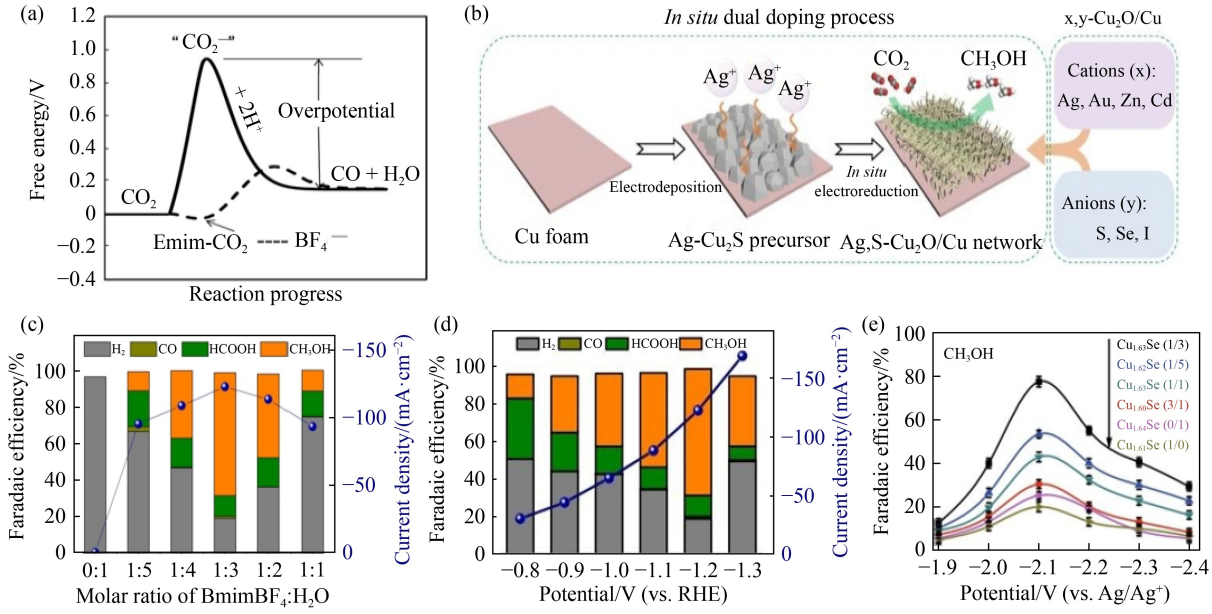

Fig. 11 Role of IL electrolytes in enhancing electrocatalytic CO_2 reduction to methanol.

(a) Schematic of free energy variation of the system during the reaction $CO_2 + 2H^+ + 2e^- \rightleftharpoons CO + H_2O$ in water or acetonitrile (solid line) or EMIM-BF_4 (dashed line) (reproduced with permission from Rosen et al. [114], copyright 2011, AAAS Publishers); (b) schematic diagram of the *in situ* dual-doping process for preparing the *x*,*y*-Cu_2O/Cu catalysts; (c) product selectivity and current density for CO_2RR over Ag,S-Cu_2O/Cu in CO_2-saturated $BMImBF_4/H_2O$ electrolyte with different molar ratios at the potential of −1.18 V vs. RHE; (d) potential-dependent product selectivity and total current density for CO_2RR by Ag,S-Cu_2O/Cu electrode (reproduced with permission from Li et al. [118], copyright 2022, Springer Nature); (e) FE over $Cu_{1.63}Se$(1/3) catalyst at different applied potentials (reproduced with permission from Yang et al. [119], copyright 2019, Springer Nature).

[Bmim]BF_4 electrolyte, it achieved a methanol FE of 80.0% at 31.8 mA/cm^2. Control experiments in $NaHCO_3$ or Na_2SO_4 electrolytes yielded primarily hydrogen and trace formate, confirming the critical role of [Bmim]BF_4 in facilitating methanol formation.

This electrolyte dependence was further demonstrated using Sn-doped defective CuO (Sn_1/V_o-CuO-90) catalysts [117]. In a [Bmim]BF_4/H_2O (molar ratio 1:3) electrolyte, this system achieved an impressive methanol FE of 88.6% at 67.0 mA/cm^2. The high performance arises from synergistic effects between atomic Sn sites, CuO carriers with adjacent oxygen vacancies, and the IL electrolyte.

In a recent breakthrough, Li et al. [118] developed *in situ* dual-doped electrocatalysts (Ag,S-Cu_2O/Cu) and systematically optimized their electrolyte environment (Fig. 11(b)). Through comprehensive screening of electrolyte compositions, they demonstrated that a [$BmimBF_4$]/H_2O (1:3 molar ratio) binary system maximizes methanol production (Fig. 11(c)).

This optimal electrolyte synergizes with the catalyst's unique architecture to achieve a methanol FE of 67.4% at current density up to 122.7 mA/cm^2 (Fig. 11(d)). Beyond binary systems, ternary electrolytes have emerged as advanced media for selective electrocatalytic CO_2RR to methanol. Yang et al. [119] pioneered a [Bmim]PF_6/CH_3CN/H_2O (30 wt%/65 wt%/5 wt%) ternary electrolyte coupled with a $Cu_{1.63}Se$ electrocatalyst, achieving a methanol FE of 77.6% at 41.5 mA/cm^2 (Fig. 11(e)). These works indicate that the enhanced performance is attributed to IL's dual role in promoting CO_2 mass transport via increased solubility and stabilizing key reaction intermediates, coupled with water-mediated proton delivery.

In summary, the electrolyte-catalyst co-optimization strategy establishes a promising route for efficient CO_2RR conversion, with IL-based systems demonstrating unparalleled methanol productivity under industrially viable conditions.

4.3 Photo-assisted CO_2RR to methanol

Photo-assisted strategies can enhance reactivity, selectivity, and energy utilization efficiency by synergizing light energy with thermal/electrical inputs or catalytic systems. Peng et al. [120] developed a zirconium-tungsten oxide heterostructure catalyst (Pt/(Zr-W)O_x) (Fig. 12(a)). This catalyst features three functional units that facilitate H_2O dissociation to generate active hydrogen species, CO production, and C–C coupling.

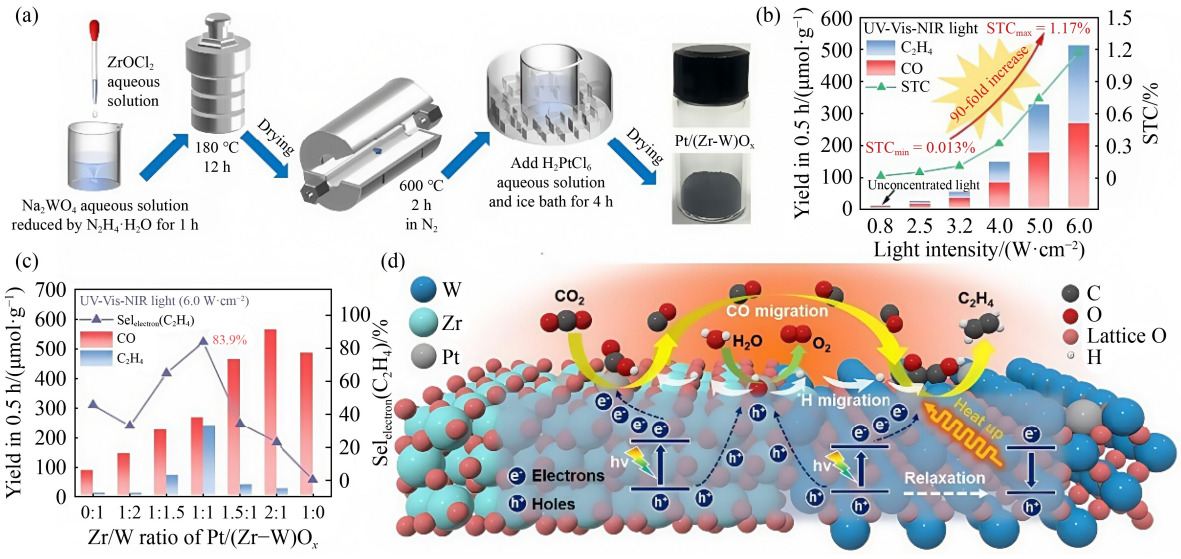

Fig. 12 Synthesis, performance, and mechanism of Pt/Zr-WO_3 photocatalyst for CO_2 hydrogenation under UV-Vis-NIR light. (a) Synthesis of Pt/(Zr–W)O_x; (b) photothermal catalytic CO_2 reduction yields of Pt/(Zr–W)O_x at different light intensities; (c) photothermal catalytic CO_2 reduction yield of Pt/(Zr–W)O_x with different Zr/W molar ratio; (d) schematic mechanism of the *H-assisted photothermal tandem catalysis on Pt/(Zr–W)O_x (reproduced with permission from Peng et al. [120], copyright 2025, ACS Catalysis Publishers).

These sites synergistically drive CO_2 conversion to diverse products. Experimental testing revealed that the yield of C_2H_4 reached 242 μmol/g after 0.5 h of concentrated solar irradiation, with 83.9% electron selectivity and 1.17% solar-to-chemical efficiency. This represents a 90-fold enhancement compared to non-concentrated conditions (Figs. 12(b) and 12(c)). The study proposed a mechanism of photothermal tandem catalysis, providing a new concept for designing efficient tandem photocatalysts (Fig. 12(d)). Complementarily, Si et al. [121]'s Ni single-atom-induced dioxygen vacancy TiO_2 photocatalyst also achieved efficient conversion of CO_2 to C_2H_4. This catalyst has a microstructure consisting of Ti-O_v(2f)-Ni-O_v(3f)-Ti, where the dioxygen vacancies work together to promote the involvement of *CO in C−C coupling. Additionally, CO_2 reduction to carbon monoxide and methane has been effectively achieved by constructing composites, depositing Pt and Au, and loading Ni [122–124].

In electrocatalytic CO_2RR to methanol, photo-assisted electrocatalysis shows unique advantages in energy conversion by combining light and electric energy [125]. This approach significantly reduces overpotentials while enhancing methanol efficiency and selectivity. Compared to conventional electrocatalysis, photoelectrocatalytic systems exhibit superior competitiveness in energy utilization, operational conditions, and product diversity, offering a viable pathway toward sustainable methanol production [126].

Currently, significant advances have been made in photoelectrocatalysis using $CuInS_2$ and Cu_2O materials. Yuan et al. demonstrated methanol production on $CuInS_2$ thin film electrodes, revealing that the methanol yield depends critically on crystal size and composition of $CuInS_2$ [127]. Subsequently, they developed an electrodeposited Cu_2O electrode [128], which exhibited strong light absorption in the visible light range of 400–550 nm (Fig. 13(a)). Studies show that the catalytic effect correlates directly with the Cu_2O crystal surface, with methanol FE reaching 29.1% under optimal conditions.

While $CuInS_2$ and Cu_2O semiconductors have excellent optical properties, their inherent catalytic activity remains limited. To address this, composite electrodes have been developed for photo-assisted CO_2RR to methanol. Yuan et al. [129] engineered CFO/CIS thin-film photoelectrodes by depositing $CuFeO_2$ nanoparticles onto $CuInS_2$ via differential pulse voltammetry (DPV). This heterostructure demonstrated superior CO_2RR performance, yielding methanol at rates three times higher than bare CuInS at an overpotential of 0.17 V, while also co-producing ethanol. The enhanced activity originates from surface Cu enrichment and suppressed electron-hole recombination.

In another study, Foster et al. [130] proposed an innovative 'catalytic mismatch' strategy by integrating a photocatalyst and an electrocatalyst to prepare a $CuInSe_2/Ni_3Al + TiO_2$ composite electrode (Fig. 13(b)). This composite achieved a FE of 25% for methanol production under optimal conditions (Fig. 13(c)), which

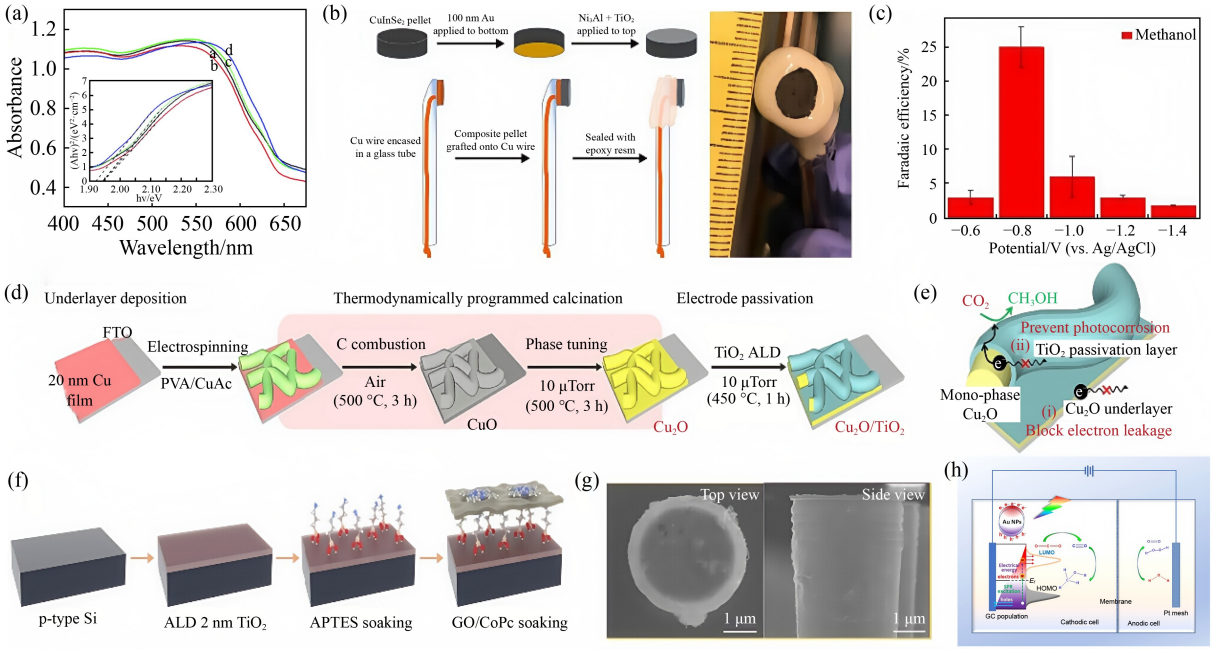

Fig. 13 Illustration of the design, fabrication, and performance evaluation of a photoelectrode system for CO_2 reduction, including optical characterization, synthesis steps, structural features, and proposed reaction mechanism.

(a) UV-vis spectra and bandgap (inset) of Cu_2O foam electrodesfrom various bath pH (reproduced with permission from Yuan et al. [128], copyright 2017, RSC Publishers); (b) fabrication of the $CuInSe_2/Ni_3Al + TiO_2$ electrode configuration; (c) Faradaic efficiencies for photoelectrochemical CO_2 reduction to methanol reported at various operating potentials (reproduced with permission from Kang et al. [130], copyright 2020, ACS Publishers); (d) fabrication scheme of hierarchically structured photocathode consisting of underlayer deposition, thermodynamically programmed calcination, and electrode passivation; (e) schematic of the hierarchical structure of the Cu_2O nanofiber electrode with a Cu_2O underlayer and a TiO_2 passivation layer (reproduced with permission from Kang et al. [131], copyright 2018, ACS Publishers); (f) illustration of STA-GO/CoPc assembly procedure (reproduced with permission from Shang et al. [132], copyright 2022, Wiley Publishers); (g) top-view and side-view SEM images of a single SMA-CFx pillar coated with CNT/CoPc-NH_2 (reproduced with permission from Shang et al. [133], copyright 2024, ACS Publishers); (h) proposed mechanism of SPR-mediated CO_2ER under illumination (reproduced with permission from Lu et al. [134], copyright 2020, ACS Publishers).

is 25 times higher than pure Ni_3Al catalyst. Kang et al. [131] further identified the kinetic processing window for single-phase Cu_2O synthesis through theoretical modeling. Guided by these calculations, they synthesized a layered photoelectrode consisting of a Cu_2O thin-film substrate, single-phase Cu_2O nanofibers, and a TiO_2 passivation layer. This structured photoelectrode demonstrated high CO_2 reduction and methanol selectivity in aqueous electrolyte.

Si and Au have demonstrated significant promise in photoelectrocatalysis due to their unique optoelectronic properties. Kang et al. [131] prepared a Co phthalocyanine-modified Si photoelectrode (STA-GO/CoPc) (Fig. 13(d)), consisted of p-type silicon, TiO_2, (3-aminopropyl) triethoxysilane, and GO/CoPc (Fig. 13(e)). This pioneering molecular-modified photoelectrode achieved CO_2RR-to-methanol conversion. Further optimization of semiconductor/catalyst interfaces led to the development of a micropillar array and coated with a superhydrophobic fluorocarbon layer (Figs. 13(f) and 13(g)) [132,133]. This architecture achieved a FE of approximately 20% under simulated sunlight by enhancing mass transport and light trapping.

In another study, Lu et al. [134] exploited the excellent electrocatalytic and light absorption properties of Au nanoparticles (Au NPs) for efficient photoelectrocatalytic CO_2RR to methanol using a surface plasmon resonance (SPR)-mediated method (Fig. 13(h)). They systematically investigated how Au NPs size influences current density and FE, alongside the influence of light wavelength and intensity on methanol selectivity. Optimal performance was achieved with 20.2 nm Au NPs on glassy carbon electrodes under 520 nm illumination (120 mW/cm^2), yielding a methanol FE of 52% at −0.8 V vs. RHE. Mechanistic analysis confirmed that plasmon-derived high-energy electrons critically enhance CO_2 activation, driving both conversion efficiency and methanol selectivity. To date, a diverse range of high-performance photoelectrode materials have demonstrated efficacy for efficient CO_2RR to methanol [135,136].

Photo-, electro-, and thermal multi-energy assistance strategies can enhance electrochemical methanol produc-

tion by overcoming the thermodynamic limitations of single electrochemical approaches, while also exhibiting promising efficiency and selectivity. Nevertheless, exploring the theoretical efficiency limits of methanol synthesis under multi-field coupling remains a fundamental challenge. Establishing dynamic efficiency models faces several obstacles, including the complex and unquantified synergies among different energy forms, the absence of a unified theoretical framework across distinct catalytic systems, and the need to bridge microscopic charge carrier behavior with macroscopic reactor performance. Therefore, establishing an "energy input-charge carrier migration-catalytic site activation" framework will be essential to delineate the theoretical efficiency boundaries of methanol synthesis under multi-field coupling conditions. Advancing research on multi-energy-assisted strategies and constructing dynamic efficiency models have thus become key priorities for future studies.

5 *In situ* research methods

In studying structure-activity relationships, *in situ* research methods are indispensable. *In situ* Raman spectroscopy, for instance, enables effective detection of dynamic changes in surface species and reaction intermediates on catalysts. Based on the principle of inelastic scattering of molecular vibrations, this technique is applicable in aqueous solutions and achieves signal amplification through surface-enhanced Raman scattering (SERS) technology. In the context of CO_2 reduction, it plays a crucial role in identifying key intermediates such as *CO, *CHO, and *CH_3O, thereby clarifying reaction mechanisms and pathways. Typically, CO_2 undergoes initial activation through electron acquisition at the catalyst surface, followed by a series PCET steps that generate various intermediates. Furthermore, this technique offers some capacity to monitor changes in the oxidation state of the catalyst. However, it remains limited by sensitivity and spatial resolution constraints, which represent key challenges for future technological advancement [137,138].

A variety of other *in situ* techniques are also widely employed to complement mechanistic understanding. FTIR offers detailed observation of reaction intermediates by detecting their characteristic vibrational modes, which is essential for identifying transient species under operational conditions. X-ray photoelectron spectroscopy (XPS) provides quantitative analysis of surface composition and chemical states of catalysts, allowing researchers to track oxidation state changes and adsorbate binding during reaction. XAS, including both X-ray absorption near edge structure (XANES) and extended X-ray absorption fine structure (EXAFS), offers element-specific insights into the local electronic structure and coordination environment of active sites. Furthermore, complementary methods such as online mass spectrometry (MS) enable real-time gas and liquid product analysis, electrochemical impedance spectroscopy (EIS) probes interfacial charge transfer and reaction kinetics, and *in situ* electron microscopy provides visual assessment of morphological and structural changes at the nanoscale. The integrated application of these techniques allows for a multidimensional understanding of catalytic mechanisms and material behavior under realistic working conditions.

6 Techno-economic analysis (TEA)

Comprehensive techno-economic assessments of electrocatalytic CO_2-to-methanol conversion reveal substantial commercialization barriers [139–142]. In addition to conventional routes, Adnan et al. systematically evaluated three emerging power-to-methanol pathways: single-step CO_2 electrolysis to methanol; two-step synthesis via water electrolysis coupled with CO_2 hydrogenation; and three-step synthesis combining water electrolysis, CO_2-to-CO electrolysis, and methanol synthesis (Fig. 14(a)) [139]. Their analysis demonstrates that, under current conditions, none of these routes are economically viable, exhibiting levelized costs of $860−1585 per ton of methanol, approximately 2 to 4 times higher than prevailing market prices ($300−500/ton). However, future scenarios with electricity costs below 3 cents/kWh could reduce production costs to $430−435 per ton, making them competitive. Crucially, cradle-to-gate lifecycle analysis indicates that climate benefits only materialize when grid emission intensity falls below 130 g CO_2/kWh. When powered exclusively by wind or nuclear energy, all three pathways achieve annual net-negative emissions of 170000–195000 tons of CO_2.

While economically promising under optimistic projections, only the two-step process currently possesses the technical maturity for industrial-scale implementation. Consequently, critical performance targets are established for CO_2 electrolysis under future low-cost electricity scenarios (3 cents/kWh): current densities exceeding 130 mA/cm^2 for CO_2-to-methanol and 360 mA/cm^2 for CO_2-to-CO conversion, alongside energy efficiencies above 40%. Meeting these thresholds would enable commercial viability for single-step and three-step pathways.

Complementing this analysis, Chang et al. [140] developed a comprehensive lifecycle assessment framework for ionic liquid-mediated CO_2 electrolysis to

methanol. The generally proposed industrial route for electrocatalytic CO_2RR to methanol, applicable to both studies, is shown in Fig. 14(b). Their sensitivity analysis identified FE, electricity costs, and cell voltage as pivotal economic determinants. The study confirms dual advantages over conventional coal-derived methanol: an 11.67% cost reduction under optimal parameters, and net-negative emissions when renewable-powered-sequestering 1.29 kg CO_2 per kg methanol produced.

Currently, industrial methanol production relies predominantly on syngas conversion. As illustrated in Fig. 15(a), raw materials such as coal and natural gas are used, with a gasifier generating syngas at high temperatures. This syngas is subsequently converted to crude methanol in a synthesis tower. After impurities are removed by a purification unit, the methanol is further refined by a separator and a distillation tower before being stored.

Analysis of conventional methanol production costs (Fig. 15(b-I)) is based on current industry data. Energy

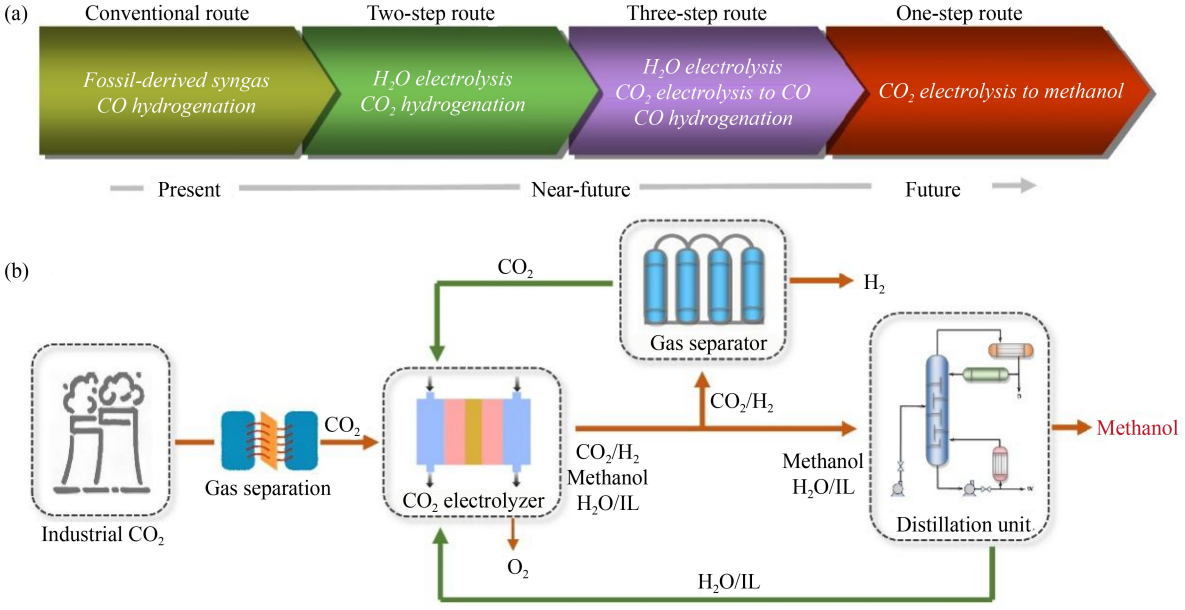

Fig. 14 Schematic representation of different technological routes for methanol production.
(a) Comparison of four methanol synthesis routes; (b) a representative industrial route for electrocatalytic CO_2RR to methanol.

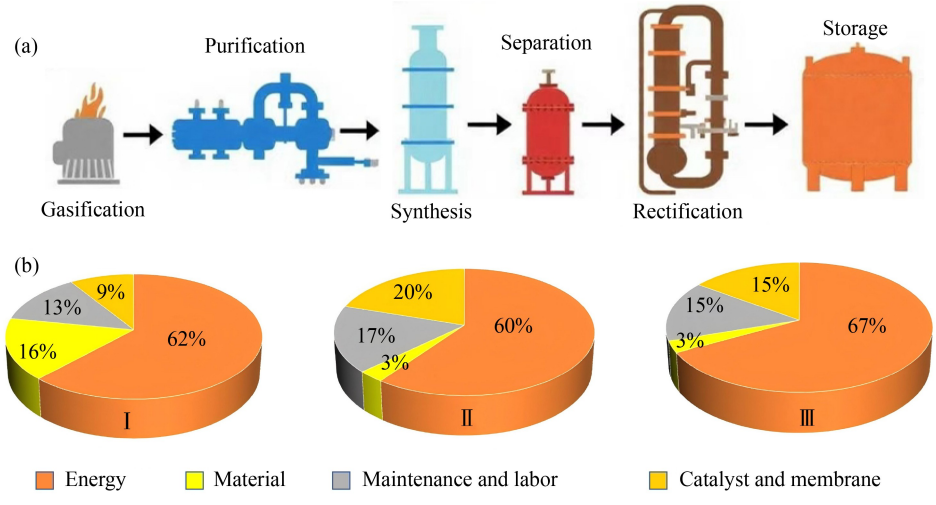

Fig. 15 Overview of the biofuel production process and the corresponding cost distribution across different production pathways.
(a) Industrial methanol production process; (b) economic share of methanol production components (I, II and III corresponding to industrial, H-cell and flow cell, respectively).

cost ranges from \$115.9 to \$154.6 per ton, calculated from coal prices of \$82.8− 96.6 per /ton at a consumption rate of \$1.4−\$1.6 tons of coal per ton of methanol. Raw material cost falls between \$29.9 and \$39.3 per ton. Maintenance and labor expenses amount to \$24.0−31.5 per ton, based on a 10000-ton production line over 20 years, plus labor costs. The catalyst cost is estimated at \$16.0−20.9 per ton, based on a catalyst price of \$11000 per ton and an amortization period of 3 to 5 years. Altogether, these components yield a total production cost of \$185.8−246.3 per ton.

For electrocatalytic CO_2-to-methanol conversion, cost projections were derived from optimal performance data of H-cells and flow cells in Table 1 (Fig. 15(b-II, b-III)) [82]. Both systems assume an industrial electricity price of \$0.07 per kWh. Considering their respective current densities, operating voltages, and methanol FE, electricity costs were calculated at \$1.65 per kg and \$1.54 per kg, respectively. Industrial CO_2 capture costs range from \$30−50 per ton, and each kilogram of methanol produced consumes about 1.375 kg of CO_2, with a feedstock cost of \$0.04−0.07 per kg. Maintenance and labor costs, including equipment investment, maintenance, operation, and supervision, are estimated to be \$0.47 and \$0.35 per kg. The resulting catalyst costs were estimated at \$50 per g, with usage amounts and lifetimes varying between the two cell types. Including membrane costs, this amounts to \$0.56 and \$0.33 per kg. Consequently, total estimated cost reach \$2.75 and \$2.29 per kg for these electrocatalytic routes.

Comparative analysis demonstrates that while electrocatalytic CO_2 conversion offers environmental advantages, its production cost (\$2290–2750 per ton) substantially exceeds conventional syngas methods (\$186–246 per ton). This economic disparity currently limits the technology to laboratory-scale and specialized applications. Future breakthroughs in catalyst efficiency, system lifetime, and reductions in green power cost are essential to make the electrocatalytic route commercially viable.

7 Summary and outlook

Compared to traditional syngas-based methanol production, electrocatalytic CO_2RR to methanol represents a promising research direction aligned with environmental protection and resource sustainability goals. This approach utilizes excess CO_2 to mitigate global warming while producing methanol through a green, sustainable process. This review summarizes the current status of this technology, covering fundamental reduction pathways, innovative reactor designs, and catalytic systems, including mono-/bimetallic, molecular, and carbon-based materials, with a particular emphasis on structure-activity relationships governing methanol selectivity. It also discusses performance-enhancing strategies such as IL electrolytes and photo-assisted activation, alongside techno-economic analyses. Nevertheless, further research is essential in this promising field, as highlighted below.

Catalysts play a pivotal role in electrocatalytic CO_2RR to methanol. Both metallic and molecular catalysts demonstrate promising methanol selectivity. However, their activity and selectivity remain far below industrial requirements. Moreover, maintaining long-term catalyst stability under operational conditions is a significant challenging. Future research should focus on designing sophisticated bimetallic and molecular composite catalysts to enhance reaction kinetics and durability overall performance.

IL electrolytes offer significant advantages for electrocatalytic CO_2RR to methanol. By tailoring anions-cation combinations, ion mobility and catalytic efficiency can be enhanced. The addition of co-catalysts such as pyridine further reduces overpotential and enhances methanol selectivity. Most current studies on CO_2RR-to-methanol utilize commercially available ILs. Future research should focus on exploring functionalized, task-specific ILs to develop high-performance, stable electrolyte systems.

Photo-assisted electrocatalysis leverages light energy to enhance CO_2RR efficiency. Materials such as $CuInS_2$, Cu_2O, Si, and Au have demonstrated promising methanol conversion efficiencies. Future research priorities include exploring low-cost, earth-abundant alternatives, enhancing photoelectrode durability, and optimizing their integration with other system components.

In situ characterization techniques are essential for understanding structure-activity relationships. *In situ* FTIR enables detailed monitoring of reaction intermediates while techniques like *in situ* XRD, XPS, and XAS provide insights into catalyst surface composition and local structure. Additionally, complementary *in situ* techniques such as mass spectrometry (MS), electrochemical impedance spectroscopy (EIS), and electron microscopy are also strategically employed to gain a multidimensional understanding of catalytic mechanisms.

In summary, this review provides a comprehensive overview of recent advances in electrocatalytic CO_2 reduction to methanol, offering a holistic perspective to guide future research. To realize commercially viable electrocatalytic methanol synthesis, future efforts should focus on advancing the rational design of novel catalysts and electrolytes, the development of innovative multi-energy assistance strategies, and in-depth mechanistic studies.

Acknowledgements This work was financially supported by the National Key Laboratory of High-Efficiency Flexible Coal Power Generation and Carbon Capture Utilization and Storage and China Huaneng Group, China (Grant No. HNKJ24-H13)

Competing Interests The authors declare that they have no known competing financial interests or personal relationships that could have appeared to influence the work reported in this paper.

References

1. Olah G A, Goeppert A, Prakash G K S. Chemical recycling of carbon dioxide to methanol and dimethyl ether: From greenhouse gas to renewable, environmentally carbon neutral fuels and synthetic hydrocarbons. Journal of Organic Chemistry, 2009, 74(2): 487–498
2. Solomon S, Plattner G K, Knutti R, et al. Irreversible climate change due to carbon dioxide emissions. Proceedings of the National Academy of Sciences of the United States of America, 2009, 106(6): 1704–1709
3. Strauss B H. Rapid accumulation of committed sea-level rise from global warming. Proceedings of the National Academy of Sciences of the United States of America, 2013, 110(34): 13699–13700
4. Zeebe R E. Time-dependent climate sensitivity and the legacy of anthropogenic greenhouse gas emissions. Proceedings of the National Academy of Sciences of the United States of America, 2013, 110(34): 13739–13744
5. Zhan X, Fan X, Li W, et al. Coupled metal atomic pairs for synergistic electrocatalytic CO_2 reduction. Matter, 2024, 7(12): 4206–4232
6. Jia S, Dong M, Zhu Q, et al. Electrochemical conversion of CO_2 via C−X bond formation: recent progress and perspective. Chemical Synthesis, 2024, 4: 60
7. Wang Z, Zhang Y, Jiang L, et al. Post-modified porous aromatic frameworks for carbon dioxide capture. Chemical Synthesis, 2024, 4: 40
8. Masoumi Z, Tayebi M, Tayebi M, et al. Electrocatalytic reactions for converting CO_2 to value-added products: Recent progress and emerging trends. International Journal of Molecular Sciences, 2023, 24(12): 9952
9. Yao Z, Cheng H, Xu Y, et al. Hydrogen radical-boosted electrocatalytic CO_2 reduction using Ni-partnered heteroatomic pairs. Nature Communications, 2024, 15(1): 9881
10. Dong X, Sun X, Jia S, et al. Electrochemical CO_2 reduction to C_{2+} products with ampere-level current on carbon-modified copper catalysts. Acta Physico-Chimica Sinica, 2025, 41(3): 100024
11. Soodi S, Zhang J J, Zhang J, et al. Selective electroreduction of CO_2 to C_{2+} products on cobalt decorated copper catalysts. Chemical Synthesis, 2024, 4: 44
12. Wang S, Zhou S, Ma Z, et al. Oxygen-substituted porous C_2N frameworks as efficient electrocatalysts for carbon dioxide electroreduction. Angewandte Chemie International Edition, 2025, 64: e202501896
13. Niu Z Z, Chi L P, Wu Z Z, et al. CO_2-assisted formation of grain boundaries for efficient CO–CO coupling on a derived Cu catalyst. National Science Open, 2023, 2(2): 20220044
14. Choi C, Kwon S, Cheng T, et al. Highly active and stable stepped Cu surface for enhanced electrochemical CO_2 reduction to C_2H_4. Nature Catalysis, 2020, 3(10): 804–812
15. Chen X, Chen J, Alghoraibi N M, et al. Electrochemical CO_2-to-ethylene conversion on polyamine-incorporated Cu electrodes. Nature Catalysis, 2020, 4(1): 20–27
16. Sharma R K, Yadav S, Dutta S, et al. Silver nanomaterials: Synthesis and (electro/photo) catalytic applications. Chemical Society Reviews, 2021, 50(20): 11293–11380
17. Zhang R, Cao J, Wang W, et al. Research on design strategies and sensing applications of energy storage system based on renewable methanol fuel. Results in Engineering, 2023, 20: 101439
18. Zhang W, Song M, Yang Q, et al. Current advance in bioconversion of methanol to chemicals. Biotechnology for Biofuels, 2018, 11: 260
19. Kim J, Masoumilari S, Park Y, et al. Advancements in the electrochemical upcycling of waste plastics into high-value products. Crystals, 2025, 15(4): 293
20. DuanMu J W, Wu Z Z, Gao F Y, et al. Investigation and mitigation of carbon deposition over copper catalyst during electrochemical CO_2 reduction. Precision chemistry, 2024, 2(4): 151–160
21. Tayebi M, Masoumi Z, Seo B, et al. Production of H_2 and glucaric acid using electrocatalyst glucose oxidation by the Ta NiFe LDH electrode. ACS Applied Materials & Interfaces, 2024, 16(20): 26107–26120
22. Chi L P, Zhang Y C, Niu Z Z, et al. Acidic CO_2 electrolysis with near-ideal selectivity and carbon efficiency enabled by overcoming its inherent trade-off. Angewandte Chemie, 2025, 64(25): e202503539
23. Wang Y, Chen L, Li G, et al. Molecular modification strategies for enhancing CO_2 electroreduction. Molecules, 2025, 30(14): 3038
24. Goeppert A, Czaun M, Jones J P, et al. Recycling of carbon dioxide to methanol and derived products–closing the loop. Chemical Society Reviews, 2014, 43(23): 7995–8048
25. Peng L, Zhang Y, He R, et al. Research advances in electrocatalysts, electrolytes, reactors and membranes for the electrocatalytic carbon dioxide reduction reaction. Acta Physico-Chimica Sinica, 2023, 39: 2302037
26. Back S, Kim H, Jung Y. Selective heterogeneous CO_2 electroreduction to methanol. ACS Catalysis, 2015, 5(2): 965–971
27. Zhang S, Jing X, Wang Y, et al. Towards carbon-neutral methanol production from carbon dioxide electroreduction. ChemNanoMat: Chemistry of Nanomaterials for Energy, Biology and More, 2021, 7(7): 728–736
28. Albo J, Alvarez-Guerra M, Castaño P, et al. Towards the electrochemical conversion of carbon dioxide into methanol.

Green Chemistry, 2015, 17(4): 2304–2324
29. Lee H, Park N, Kong T H, et al. Advancements in electrochemical methanol synthesis from CO_2: Mechanisms and catalyst developments. Nano Energy, 2024, 130: 110099
30. He H, Ren Y, Zhu Y H, et al. Continuous flow photothermal catalytic CO_2 reduction: Materials, mechanisms, and system design. ACS Catalysis, 2025, 15(12): 10480–10520
31. Yao C L, Li J C, Gao W, et al. An integrated design with new metal-functionalized covalent organic frameworks for the effective electroreduction of CO_2. Chemistry, 2018, 24(43): 11051–11058
32. Sun X, Araujo R B, Dos Santos E C, et al. Advancing electrocatalytic reactions through mapping key intermediates to active sites via descriptors. Chemical Society Reviews, 2024, 53(14): 7392–7425
33. Lin R, Guo J, Li X, et al. Electrochemical reactors for CO_2 conversion. Catalysts, 2020, 10(5): 473
34. Hernandez-Aldave S, Andreoli E. Fundamentals of gas diffusion electrodes and electrolysers for carbon dioxide utilisation: Challenges and opportunities. Catalysts, 2020, 10(6): 713
35. Chandrashekar S, Geerlings H, Smith W A. Assessing silver palladium alloys for electrochemical CO_2 reduction in membrane electrode assemblies. ChemElectroChem, 2021, 8(23): 4515–4521
36. He H, Ren Y, Lan S, et al. Cross-scale construction of photothermal synergistic catalytic systems: Mechanistic insights from single atoms, clusters to nanoparticles and energy conversion applications. Applied Catalysis B: Environment and Energy, 2025, 378: 125623
37. Ren Y, Lan S, Zhu Y H, et al. Concentrated solar-driven catalytic CO_2 reduction: From fundamental research to practical applications. ChemSusChem, 2025, 18(10): e202402485
38. Shajirati Y, Momeni M M, Tayebi M, et al. Facile synthesis of interlaced flower-like layered double hydroxides grown on porous CoMoP as a highly efficient electrocatalyst for hydrogen evolution reaction. Energy, 2023, 278: 127840
39. Zhu Y, Cui X, Liu H, et al. Tandem catalysis in electrochemical CO_2 reduction reaction. Nano Research, 2021, 14(12): 4471–4486
40. Lin S, Diercks C S, Zhang Y B, et al. Covalent organic frameworks comprising cobalt porphyrins for catalytic CO_2 reduction in water. Science, 2015, 349(6253): 1208–1213
41. Xue D, Xia H, Yan W, et al. Defect engineering on carbon-based catalysts for electrocatalytic CO_2 reduction. Nano-Micro Letters, 2021, 13(1): 5
42. Al-Rowaili F N, Jamal A, Ba Shammakh M S, et al. A review on recent advances for electrochemical reduction of carbon dioxide to methanol using metal-organic framework (MOF) and non-MOF catalysts: Challenges and future prospects. ACS Sustainable Chemistry & Engineering, 2018, 6(12): 15895–15914
43. Guzmán H, Russo N, Hernández S. CO_2 valorisation towards alcohols by Cu-based electrocatalysts: Challenges and perspectives. Green Chemistry, 2021, 23(5): 1896–1920
44. Xue Q, Qi X, Li K, et al. DFT study of CO_2 reduction reaction to CH_3OH on low-index Cu surfaces. Catalysts, 2023, 13(4): 722
45. Gao W, Xu Y, Fu L, et al. Experimental evidence of distinct sites for CO_2-to-CO and CO conversion on Cu in the electrochemical CO_2 reduction reaction. Nature Catalysis, 2023, 6(10): 885–894
46. Murthy P S, Liang W, Jiang Y, et al. Cu-Based nanocatalysts for CO_2 hydrogenation to methanol. Energy & Fuels, 2021, 35(10): 8558–8584
47. Roy A, Jadhav H S, Gil Seo J. Cu_2O/CuO electrocatalyst for electrochemical reduction of carbon dioxide to methanol. Electroanalysis, 2021, 33(3): 705–712
48. Hirunsit P, Soodsawang W, Limtrakul J. CO_2 electrochemical reduction to methane and methanol on copper-based alloys: Theoretical insight. Journal of Physical Chemistry C, 2015, 119(15): 8238–8249
49. Yu H, Han X, Hua Z, et al. Modulating electronic properties of carbon for selective electrochemical reduction of CO_2 to methanol on Cu_3P@C. ACS Catalysis, 2024, 14(17): 12783–12791
50. Vasileff A, Zhi X, Xu C, et al. Selectivity control for electrochemical CO_2 reduction by charge redistribution on the surface of copper alloys. ACS Catalysis, 2019, 9(10): 9411–9417
51. Kothandaraman J, Goeppert A, Czaun M, et al. Conversion of CO_2 from air into methanol using a polyamine and a homogeneous ruthenium catalyst. Journal of the American Chemical Society, 2016, 138(3): 778–781
52. Chen Q, Zhao L, Zhao X, et al. Rh_4 cluster supported on the In_2O_3(111) surface for enhancing the turnover frequency of CO_2 hydrogenation to methanol: The application of energetic span model. Separation and Purification Technology, 2024, 329: 125107
53. Cai Z, Dai J, Li W, et al. Pd supported on MIL-68 (In)-derived In_2O_3 nanotubes as superior catalysts to boost CO_2 hydrogenation to methanol. ACS Catalysis, 2020, 10(22): 13275–13289
54. Sun K, Shen C, Zou R, et al. Highly active Pt/In_2O_3-ZrO_2 catalyst for CO_2 hydrogenation to methanol with enhanced CO tolerance: The effects of ZrO_2. Applied Catalysis B: Environmental, 2023, 320: 122018
55. Zhang W, Qin Q, Dai L, et al. Electrochemical reduction of carbon dioxide to methanol on hierarchical Pd/SnO_2 nanosheets with abundant Pd–O–Sn interfaces. Angewandte Chemie International Edition, 2018, 57(30): 9475–9479
56. Zhu N, Zhang X, Chen N, et al. Integration of MnO_2 nanosheets with Pd nanoparticles for efficient CO_2 electroreduction to methanol in membrane electrode assembly electrolyzers. Journal of the American Chemical Society, 2023, 145(45): 24852–24861
57. Sun H, Li D, Min Y, et al. Hierarchical palladium–copper–silver porous nanoflowers as efficient electrocatalysts for CO_2 reduction to C_{2+} products. Acta Physico-Chimica Sinica, 2024, 40(6): 2307007
58. Wang X, He B, Hu Z, et al. Current advances in precious metal

core-shell catalyst design. Science and Technology of Advanced Materials, 2014, 15(4): 043502
59. Zhang B, Fan L, Ambre R B, et al. Advancing proton exchange membrane electrolyzers with molecular catalysts. Joule, 2020, 4(7): 1408–1444
60. Younus H A, Ahmad N, Ni W, et al. Molecular catalysts for CO_2 electroreduction: Progress and prospects with pincer type complexes. Coordination Chemistry Reviews, 2023, 493: 215318
61. Lei K, Yu Xia B. Electrocatalytic CO_2 reduction: From discrete molecular catalysts to their integrated catalytic materials. Chemistry, 2022, 28(30): e202200141
62. Grammatico D, Bagnall A J, Riccardi L, et al. Heterogenised molecular catalysts for sustainable electrochemical CO_2 reduction. Angewandte Chemie, 2022, 134(38): e202206399
63. Fang H, Liu G, Huang Z. Dehydrogenation of alkanes using molecular catalysts. In: Pombeiro A J L, da Silva F C G, eds. Alkane Functionalization. Bognor Regis: John Wiley & Sons Ltd, 2019, 467–483
64. Rosser T E, Hisatomi T, Sun S, et al. $La_5Ti_2Cu_{0.9}Ag_{0.1}S_5O_7$ modified with a molecular Ni catalyst for photoelectrochemical H_2 generation. Chemistry, 2018, 24(69): 18393–18397
65. Friedman A, Mizrahi M, Levy N, et al. Application of molecular catalysts for the oxygen reduction reaction in alkaline fuel cells. ACS Applied Materials & Interfaces, 2021, 13(49): 58532–58538
66. Zhao B, Han J, Liu B, et al. Hierarchical metal-organic framework nanoarchitectures for catalysis. Chemical Synthesis, 2024, 4: 41
67. Tayebi M, Masoumi Z, Lee H, et al. MOF-derived FeCoO/N-doped C bifunctional electrode for H_2 production through water and glucose electrolysis. Advanced Sustainable Systems, 2024, 8(11): 2400342
68. Shao B, Dong H, Gong Y, et al. Meta-organic framework-derived nickel nanoparticles for efficient CO_2 electroreduction in wide potential windows. Acta Physico-Chimica Sinica, 2024, 40(4): 2305026
69. Albo J, Vallejo D, Beobide G, et al. Copper-based metal-organic porous materials for CO_2 electrocatalytic reduction to alcohols. ChemSusChem, 2017, 10(6): 1100–1109
70. Zhao K, Liu Y, Quan X, et al. CO_2 electroreduction at low overpotential on oxide-derived Cu/carbons fabricated from metal organic framework. ACS Applied Materials & Interfaces, 2017, 9(6): 5302–5311
71. Boutin E, Wang M, Lin J C, et al. Aqueous electrochemical reduction of carbon dioxide and carbon monoxide into methanol with cobalt phthalocyanine. Angewandte Chemie International Edition, 2019, 58(45): 16172–16176
72. Yu S, Yamauchi H, Wang S, et al. CO_2-to-methanol electroconversion on a molecular cobalt catalyst facilitated by acidic cations. Nature Catalysis, 2024, 7(9): 1000–1009
73. Wu Y, Jiang Z, Lu X, et al. Domino electroreduction of CO_2 to methanol on a molecular catalyst. Nature, 2019, 575(7784): 639–642
74. Rooney C L, Lyons M, Wu Y, et al. Active sites of cobalt phthalocyanine in electrocatalytic CO_2 reduction to methanol. Angewandte Chemie, 2024, 136(2): e202310623
75. Zhu Q, Rooney C L, Shema H, et al. The solvation environment of molecularly dispersed cobalt phthalocyanine determines methanol selectivity during electrocatalytic CO_2 reduction. Nature Catalysis, 2024, 7(9): 987–999
76. Cheon S, Li J, Wang H. *In situ* generated CO enables high-current CO_2 reduction to methanol in a molecular catalyst layer. Journal of the American Chemical Society, 2024, 146(23): 16348–16354
77. Li J, Shang B, Gao Y, et al. Mechanism-guided realization of selective carbon monoxide electroreduction to methanol. Nature Synthesis, 2023, 2(12): 1194–1201
78. Ren X, Zhao J, Li X, et al. In-situ spectroscopic probe of the intrinsic structure feature of single-atom center in electrochemical CO/CO_2 reduction to methanol. Nature Communications, 2023, 14(1): 3401
79. Chan T, Kong C J, King A J, et al. Role of mass transport in electrochemical CO_2 reduction to methanol using immobilized cobalt phthalocyanine. ACS Applied Energy Materials, 2024, 7(8): 3091–3098
80. Guo T, Wang X, Ma C, et al. Electrochemical CO_2 reduction by cobalt (ii) 2,9,16,23-tetra (amino) phthalocyanine: Enhancement effect of active sites toward methanol formation. Energy & Fuels, 2024, 38(17): 16638–16656
81. Zhang C, Follana-Berná J, Dragoe D, et al. Cobalt tetracationic 3, 4-pyridinoporphyrazine for direct CO_2 to methanol conversion escaping the co intermediate pathway. Angewandte Chemie International Edition, 2024, 63(50): e202411967
82. Li J, Zhu Q, Chang A, et al. Molecular-scale CO spillover on a dual-site electrocatalyst enhances methanol production from CO_2 reduction. Nature Nanotechnology, 2025, 20(4): 515–522
83. Song Y, Guo P, Ma T, et al. Ultrathin, cationic covalent organic nanosheets for enhanced CO_2 electroreduction to methanol. Advanced Materials, 2024, 36(17): 2310037
84. Hutchison P, Smith L E, Rooney C L, et al. Proton-coupled electron transfer mechanisms for CO_2 reduction to methanol catalyzed by surface-immobilized cobalt phthalocyanine. Journal of the American Chemical Society, 2024, 146(29): 20230–20240
85. Zhang J, Pham T H M, Xi S, et al. Low CO_2 mass transfer promotes methanol and formaldehyde electrosynthesis on cobalt phthalocyanine. Journal of Materials Chemistry. A, Materials for Energy and Sustainability, 2024, 12(45): 31547–31556
86. Yao L, Ding J, Cai X, et al. Unlocking the potential for methanol synthesis via electrochemical CO_2 reduction using CoPc-based molecular catalysts. ACS Nano, 2024, 18(33): 21623–21632
87. Jarvis A G. Designer metalloenzymes for synthetic biology: enzyme hybrids for catalysis. Current Opinion in Chemical Biology, 2020, 58: 63–71
88. Li X, Fu C, Luo L, et al. Design of enzyme-metal hybrid catalysts for organic synthesis. Cell Reports. Physical Science, 2022, 3(3): 100742

89. Kalita P, Basumatary B, Saikia P, et al. Biodiesel as renewable biofuel produced via enzyme-based catalyzed transesterification. Energy Nexus, 2022, 6: 100087
90. Avhad M R, Marchetti J M. Uses of enzymes for biodiesel production. In: Hosseini M, ed. Advanced Bioprocessing for Alternative Fuels, Biobased Chemicals, and Bioproducts. Cambridge: Woodhead Publishing, 2019, 135–152
91. Zhang B, Shi J, Chu Z, et al. Lysine-modulated synthesis of enzyme-embedded hydrogen-bonded organic frameworks for efficient carbon dioxide fixation. Chemical Synthesis, 2023, 3: 5
92. Gu Y, Li S, Li M, et al. Recent advances in g-C_3N_4-based photo-enzyme catalysts for degrading organic pollutants. RSC Advances, 2023, 13(2): 937–947
93. El-Zahab B, Donnelly D, Wang P. Particle-tethered NADH for production of methanol from CO_2 catalyzed by coimmobilized enzymes. Biotechnology and Bioengineering, 2008, 99(3): 508–514
94. Di Spiridione C, Aresta M, Dibenedetto A. Improving the enzymatic cascade of reactions for the reduction of CO_2 to CH_3OH in water: From enzymes immobilization strategies to cofactor regeneration and cofactor suppression. Molecules, 2022, 27(15): 4913
95. Sultana S, Sahoo P C, Martha S, et al. A review of harvesting clean fuels from enzymatic CO_2 reduction. RSC Advances, 2016, 6(50): 44170–44194
96. Schlager S, Dumitru L M, Haberbauer M, et al. Electrochemical reduction of carbon dioxide to methanol by direct injection of electrons into immobilized enzymes on a modified electrode. ChemSusChem, 2016, 9(6): 631–635
97. Zhang Z, Li J, Ji M, et al. Encapsulation of multiple enzymes in a metal-organic framework with enhanced electro-enzymatic reduction of CO_2 to methanol. Green Chemistry, 2021, 23(6): 2362–2371
98. Ma K, Yehezkeli O, Park E, et al. Enzyme mediated increase in methanol production from photoelectrochemical cells and CO_2. ACS Catalysis, 2016, 6(10): 6982–6986
99. Costentin C, Robert M, Savéant J M. Catalysis of the electrochemical reduction of carbon dioxide. Chemical Society Reviews, 2013, 42(6): 2423–2436
100. Wang W, Zhang J, Wang H, et al. Photocatalytic and electrocatalytic reduction of CO_2 to methanol by the homogeneous pyridine-based systems. Applied Catalysis A, General, 2016, 520: 1–6
101. Seshadri G, Lin C, Bocarsly A B. A new homogeneous electrocatalyst for the reduction of carbon dioxide to methanol at low overpotential. Journal of Electroanalytical Chemistry, 1994, 372(1–2): 145–150
102. Barton Cole E, Lakkaraju P S, Rampulla D M, et al. Using a one-electron shuttle for the multielectron reduction of CO_2 to methanol: kinetic, mechanistic, and structural insights. Journal of the American Chemical Society, 2010, 132(33): 11539–11551
103. Portenkirchner E, Enengl C, Enengl S, et al. A comparison of pyridazine and pyridine as electrocatalysts for the reduction of carbon dioxide to methanol. ChemElectroChem, 2014, 1(9): 1543–1548
104. Rybchenko S I, Touhami D, Wadhawan J D, et al. Study of pyridine-mediated electrochemical reduction of CO_2 to methanol at high CO_2 pressure. ChemSusChem, 2016, 9(13): 1660–1669
105. Giesbrecht P K, Herbert D E. Electrochemical reduction of carbon dioxide to methanol in the presence of benzannulated dihydropyridine additives. ACS Energy Letters, 2017, 2(3): 549–555
106. Saveant J M, Tard C. Attempts to catalyze the electrochemical CO_2-to-methanol conversion by biomimetic $2e^- + 2H^+$ transferring molecules. Journal of the American Chemical Society, 2016, 138(3): 1017–1021
107. Lim C H, Holder A M, Hynes J T, et al. Dihydropteridine/pteridine as a $2H^+/2e^-$ redox mediator for the reduction of CO_2 to methanol: A computational study. Journal of Physical Chemistry B, 2017, 121(16): 4158–4167
108. Bi J, Hou P, Liu F W, et al. Electrocatalytic reduction of CO_2 to methanol by iron tetradentate phosphine complex through amidation strategy. ChemSusChem, 2019, 12(10): 2195–2201
109. Ko H, Kim M, Hong S Y, et al. Plasma-assisted mechanochemistry to covalently bond ion-conducting polymers to Ni-rich cathode materials for improved cyclic stability and rate capability. ACS Applied Energy Materials, 2022, 5(4): 4808–4816
110. König M, Vaes J, Klemm E, et al. Solvents and supporting electrolytes in the electrocatalytic reduction of CO_2. iScience, 2019, 19: 135–160
111. Rong Y, Sang J, Che L, et al. Designing electrolytes for aqueous electrocatalytic CO_2 reduction. Acta Physico-Chimica Sinica, 2023, 39(5): 2212027
112. Moura de Salles Pupo M, Kortlever R. Electrolyte effects on the electrochemical reduction of CO_2. ChemPhysChem, 2019, 20(22): 2926–2935
113. Tan X, Sun X, Han B. Ionic liquid-based electrolytes for CO_2 electroreduction and CO_2 electroorganic transformation. National Science Review, 2022, 9(4): nwab022
114. Rosen B A, Salehi-Khojin A, Thorson M R, et al. Ionic liquid-mediated selective conversion of CO_2 to CO at low overpotentials. Science, 2011, 334(6056): 643–644
115. Sun X, Zhu Q, Kang X, et al. Molybdenum-bismuth bimetallic chalcogenide nanosheets for highly efficient electrocatalytic reduction of carbon dioxide to methanol. Angewandte Chemie, 2016, 128(23): 6883–6887
116. Lu L, Sun X, Ma J, et al. Highly efficient electroreduction of CO_2 to methanol on palladium-copper bimetallic aerogels. Angewandte Chemie, 2018, 130(43): 14345–14349
117. Guo W, Liu S, Tan X, et al. Highly efficient CO_2 electroreduction to methanol through atomically dispersed Sn coupled with defective CuO catalysts. Angewandte Chemie International Edition, 2021, 60(40): 21979–21987
118. Li P, Bi J, Liu J, et al. *In situ* dual doping for constructing efficient CO_2-to-methanol electrocatalysts. Nature Communications, 2022, 13(1): 1965
119. Yang D, Zhu Q, Chen C, et al. Selective electroreduction of

carbon dioxide to methanol on copper selenide nanocatalysts. Nature Communications, 2019, 10(1): 677

120. Peng R, Ren Y, Si Y, et al. Strong photothermal tandem catalysis for CO_2 reduction to C_2H_4 boosted by Zr-O-W interfacial H_2O dissociation. ACS Catalysis, 2025, 15(1): 1–13
121. Si Y, Li Y, Cheng M, et al. Synergistic dual-oxygen-vacancy design boosts photothermal CO_2 reduction into ethylene. Nano Energy, 2025, 138: 110838
122. He H, Ren Y, Zhang L, et al. Synergistic modulation of charge dynamics and mass transfer optimization via heterogeneous interface engineering in photothermal catalytic CO_2 reduction within continuous flow systems. Nano Energy, 2025, 142: 111290
123. Ren Y, Si Y, Du M, et al. Photothermal synergistic effect induces bimetallic cooperation to modulate product selectivity of CO_2 reduction on different CeO_2 crystal facets. Angewandte Chemie, 2024, 136(46): e202410474
124. Ren Y, Fu Y, Li N, et al. Concentrated solar CO_2 reduction in H_2O vapour with > 1% energy conversion efficiency. Nature Communications, 2024, 15(1): 4675
125. Masoumi Z, Tayebi M, Zaib Q, et al. Photo-electrochemical ep-oxidation using environmentally friendly oxidants: Overview of recent advances in efficiently designed photo-electrode. Coordination Chemistry Reviews, 2024, 503: 215641
126. Kumar B, Llorente M, Froehlich J, et al. Photochemical and photoelectrochemical reduction of CO_2. Annual Review of Physical Chemistry, 2012, 63(1): 541–569
127. Yuan J, Zheng L, Hao C. Role of pyridine in photoelectrochemical reduction of CO_2 to methanol at a $CuInS_2$ thin film electrode. RSC Advances, 2014, 4(74): 39435–39438
128. Yuan J, Wang X, Gu C, et al. Photoelectrocatalytic reduction of carbon dioxide to methanol at cuprous oxide foam cathode. RSC Advances, 2017, 7(40): 24933–24939
129. Yuan J, Gu C, Ding W, et al. Photo-electrochemical reduction of carbon dioxide into methanol at $CuFeO_2$ nanoparticle-decorated $CuInS_2$ thin-film photocathodes. Energy & Fuels, 2020, 34(8): 9914–9922
130. Foster B M, Paris A R, Frick J J, et al. Catalytic mismatching of $CuInSe_2$ and Ni_3Al demonstrates selective photoelectrochemical CO_2 reduction to methanol. ACS Applied Energy Materials, 2020, 3(1): 109–113
131. Kang H Y, Nam D H, Yang K D, et al. Synthetic mechanism discovery of monophase cuprous oxide for record high photoelectrochemical conversion of CO_2 to methanol in water. ACS Nano, 2018, 12(8): 8187–8196
132. Shang B, Rooney C L, Gallagher D J, et al. Aqueous photoelectrochemical CO_2 reduction to CO and methanol over a silicon photocathode functionalized with a cobalt phthalocyanine molecular catalyst. Angewandte Chemie International Edition, 2023, 62(4): e202215213
133. Shang B, Zhao F, Suo S, et al. Tailoring interfaces for enhanced methanol production from photoelectrochemical CO_2 reduction. Journal of the American Chemical Society, 2024, 146(3): 2267–2274
134. Lu W, Ju F, Yao K, et al. Photoelectrocatalytic reduction of CO_2 for efficient methanol production: Au nanoparticles as electrocatalysts and light supports. Industrial & Engineering Chemistry Research, 2020, 59(10): 4348–4357
135. Sayao F A, Ma X, Zanoni M V B, et al. Modulating the photoelectrocatalytic conversion of CO_2 to methanol and/or H_2O to hydrogen at a phosphorene modified Ti/TiO_2 electrode. Journal of Materials Chemistry. C, Materials for Optical and Electronic Devices, 2022, 10(31): 11276–11285
136. Fang Y, Gao Y, Wen Y, et al. Photoelectrocatalytic CO_2 reduction to methanol by molecular self-assemblies confined in covalent polymer networks. Journal of the American Chemical Society, 2024, 146(40): 27475–27485
137. Song X, Xu L, Sun X, et al. *In situ*/operando characterization techniques for electrochemical CO_2 reduction. Science China. Chemistry, 2023, 66(2): 315–323
138. Chen M, Liu D, Qiao L, et al. *In-situ*/operando Raman techniques for in-depth understanding on electrocatalysis. Chemical Engineering Journal, 2023, 461: 141939
139. Adnan M A, Kibria M G. Comparative techno-economic and life-cycle assessment of power-to-methanol synthesis pathways. Applied Energy, 2020, 278: 115614
140. Chang F, Zhun G, Shi S, et al. Process assessment for electroreduction CO_2 to methanol in ionic liquid electrolyte. Chemical Industry and Engineering Progress, 2022, 41(3): 1256
141. De Luna P, Hahn C, Higgins D, et al. What would it take for renewably powered electrosynthesis to displace petrochemical processes? Science, 2019, 364(6438): eaav3506
142. Orella M J, Brown S M, Leonard M L E, et al. A general technoeconomic model for evaluating emerging electrolytic processes. Energy Technology, 2020, 8(11): 1900994
143. Biswas S, Tanaka T, Song H, et al. Highly selective methanol synthesis using electrochemical CO_2 reduction with defect-engineered Cu_{58} nanoclusters. Small Science, 2025, 5(2): 2400465
144. Wang P, Wang X, Zhang J, et al. Modulating the active sites of VS_2 by Mn doping for highly selective CO_2 electroreduction to methanol in a flow cell. ACS Applied Materials & Interfaces, 2024, 16(28): 36453–36461
145. Yang H, Wu Y, Li G, et al. Scalable production of efficient single-atom copper decorated carbon membranes for CO_2 electroreduction to methanol. Journal of the American Chemical Society, 2019, 141(32): 12717–12723
146. Huang J, Guo X, Yue G, et al. Boosting CH_3OH production in electrocatalytic CO_2 reduction over partially oxidized 5 nm cobalt nanoparticles dispersed on single-layer nitrogen-doped graphene. ACS Applied Materials & Interfaces, 2018, 10(51): 44403–44414
147. Payra S, Shenoy S, Chakraborty C, et al. Structure-sensitive electrocatalytic reduction of CO_2 to methanol over carbon-supported intermetallic PtZn nano-alloys. ACS Applied Materials & Interfaces, 2020, 12(17): 19402–19414
148. Zhang G, Wang T, Zhang M, et al. Selective CO_2 electroreduction to methanol via enhanced oxygen bonding.

Nature Communications, 2022, 13(1): 7768

149. Kong S, Lv X, Wang X, et al. Delocalization state-induced selective bond breaking for efficient methanol electrosynthesis from CO_2. Nature Catalysis, 2022, 6(1): 6–15
150. Bagchi D, Raj J, Singh A K, et al. Structure-tailored surface oxide on Cu–Ga intermetallics enhances CO_2 reduction selectivity to methanol at ultralow potential. Advanced Materials, 2022, 34(19): 2109426
151. Marcos-Madrazo A, Casado-Coterillo C, Irabien Á. Sustainable membrane-coated electrodes for CO_2 electroreduction to methanol in alkaline media. ChemElectroChem, 2019, 6(20): 5273–5282